Measurement 240 (2025) 115556

Contents lists available at ScienceDirect

Measurement

journal homepage: www.elsevier.com/locate/measurement

Modified starch as a component of environmentally friendly polymer adsorbents – from synthesis and characterization to potential application in the removal of toxic C.I. Basic Yellow 2 dye

Monika Wawrzkiewicz [a,*], Beata Podkościelna [b], Bogdan Tarasiuk [b]

[a] Department of Inorganic Chemistry, Institute of Chemical Sciences, Faculty of Chemistry, Maria Curie-Sklodowska University in Lublin, Maria Curie-Sklodowska Sq. 3, 20-031 Lublin, Poland
[b] Department of Polymer Chemistry, Institute of Chemical Sciences, Faculty of Chemistry, Maria Curie-Sklodowska University in Lublin, Maria Curie-Sklodowska Sq. 3, 20-031 Lublin, Poland

ARTICLE INFO

Keywords:
Adsorbent
Basic yellow 2
Removal
Starch
Starch modification
Textile effluents

ABSTRACT

Increasing global degradation of the aquatic environment is forcing the search for new and low-cost adsorbents of reduced toxicity, derived from natural and renewable sources. To meet these expectations, a new approach to adsorbent fabrication was developed.

The study aimed to synthesize, characterize, and apply environmentally friendly adsorbents based on poly (ethylene glycol dimethacrylate-co-vinyl acetate) (EGDMA-VA) with unmodified/modified starch (St). The first step proposed a new mechanochemical method of starch modification using thiourea (T) and potassium dihydrogen phosphate (P). Then, the functionalized starch was used to obtain polymeric microspheres. The final step involves their application for the removal of toxic C.I. Basic Yellow 2 (BY2) dye. The pristine materials and adsorbents were characterized by ATR/FT-IR and XPS, DSC, SEM/EDX, porous structure, particle size distribution, tendency to swell, and pH_{pzc}.

Adsorption batch studies of BY2 as a function of time (1–60 min), initial dye concentration (1–25 mg/L, pH=8.3), temperature (298–328 K), and competing electrolyte (5–15 g/L Na_2SO_4) and surfactant (0.1–0.5 g/L CTAB) presence were carried out. The kinetic studies were analyzed using pseudo-first order, pseudo-second order, and intraparticle diffusion models. The equilibrium studies revealed that the Freundlich isotherm model (k_F=5.62–6.56 $mg^{1-1/n}$ $L^{1/n}$) described BY2-adsorbents systems rather than Langmuir, Temkin or Dubinin-Radushkevich. Thermodynamic parameters (ΔG°, ΔH°, and ΔS°) pointed to the exothermic nature of adsorption and its spontaneousness. Importantly, the starch-modified microspheres were regenerated, too.

1. Introduction

Dyes, as organic compounds with complex molecular structures, can be found in the textile, pulp, and paper wastewaters, paints and varnishes, cosmetics, and food industries [1,2]. Their content in the effluent varies very widely from 2 to 50 %, depending on the dyeing method used and the type of product being dyed [3]. It was estimated that the content of unfixed dyes that can be discharged into the textile wastewater is: 7–20 % for acid dyes, 2–3 % for basic dyes, 5–20 % for direct dyes, 20–50 % for reactive dyes and 30–40 % for sulfur dyes [3]. In addition to dyes, wastewater from this industry may contain heavy metal ions, electrolytes (200,000–250,000 tons/year), sizing agents (80,000–100,000 tons/year), detergents (20,000–25,000 tons/year), acids (15,000–20,000 tons/year) and alkalis as well as oxidants and reducing agents [3]. The parameters of textile industry wastewater are as follows: pH 6.2 – 11.5, biochemical oxygen demand 80 – 6000 mg/L, chemical oxygen demand 150 – 12000 mg/L, total suspended solids 15 – 8000 mg/L, total dissolved solids 2900 – 3100 mg/L, surfactants 1 – 134 mg/L, chloride 1000 – 1600 mg/L, total Kjeldahl nitrogen 70 – 80 mg/L, and total chromium 1–5 mg/L [4].

Particularly hazardous to the environment are azo-type dyes, which can degrade to toxic aromatic amines under certain conditions. Dyes present in water reservoirs deteriorate their aesthetic quality, increase biochemical and chemical oxygen demand, impair photosynthesis, and inhibit plant growth. They can penetrate the food chains of fauna and humans and, through bioaccumulation, induce mutagenic and

* Corresponding author.
E-mail address: monika.wawrzkiewicz@mail.umcs.pl (M. Wawrzkiewicz).

https://doi.org/10.1016/j.measurement.2024.115556
Received 30 May 2024; Received in revised form 6 August 2024; Accepted 19 August 2024
Available online 28 August 2024

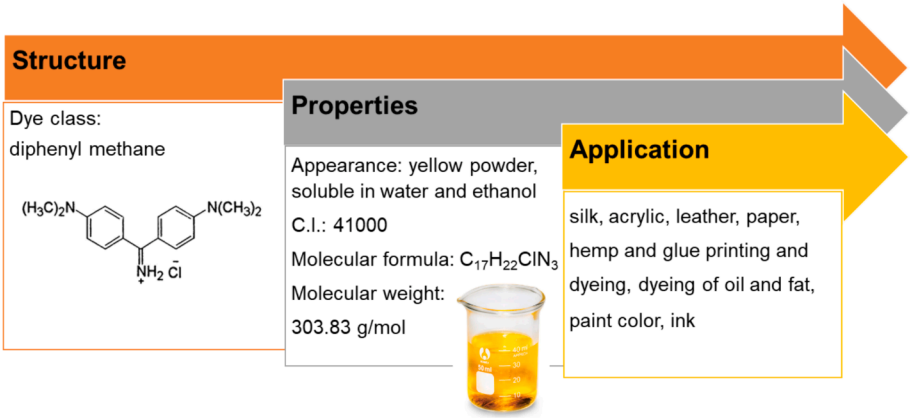

Fig. 1. Properties of C.I. Basic Yellow 2 dye.

carcinogenic processes [5]. Dyes can not only cause human contact allergic reactions such as dermatitis, rhinitis, or occupational asthma but can also cause damage to the nervous (e.g. inhibition of intracellular enzyme of the central nervous system), reproductive (e.g. cytotoxic effect on spermatozoa cells, decline in ovarian protein and glucose), immune and enzymatic (e.g. inactivation of enzymatic activities, block of enzymes such as glutathione reductase) systems and dysfunction of the kidneys (e.g. sarcoma and cancer), liver (e.g. hepatocarcinoma, an increase of serum alkaline phosphates and ϒ-glutamyl transferase) or genetic material (e.g. intercalate with the helical structure of DNA and RNA, increased frequency of micronuclei) [5].

As reported by Azevedo et al. [6], BY2 is toxic to aquatic organisms from different trophic levels and creates imbalances in a polluted ecosystem. The content of C.I. Basic Yellow 2 in the amount of 600–1300 μg/L negatively affected daphnids' reproduction and induced deformities in hydra and fish embryos. 50 % inhibition growth of aquatic organisms was observed in concentrations ≤ 800 μg/L. According to the International Agency for Research on Cancer, BY2 is classified as a compound of Group 1 (carcinogenic to humans) concerning production and as 2B (possibly carcinogenic to humans) regarding its use [6]. Determined predicted no-effect concentration (PENC) based on algae chronic effects was found to be 4.6 μg of BY2 per 1 L under the methodology adopted by the European Union [6]. Because of this, there is a need to remove dyes from wastewater before they are released into the environment.

Several methods are applied to remove dyes from contaminated waters, usually biological, chemical, or physicochemical processes [7,8]. Although the aforementioned techniques are widely used, most of them have some drawbacks and limitations, among which are incomplete removal of toxic substances/low efficiency, long reaction time, production of non-biodegradable by-products and toxic sludge, significant energy consumption, and process costs. The efficiency of biological dye removal methods ranges from 76 to 90.1 %, and chemical methods from 88 to 99 % [9]. Considering the concept of sustainable socio-economic development, which is to minimize the generated pollution, control water consumption, and recover possible substances, it is necessary to choose the most efficient method or use a combination of the mentioned methods. The adsorption technique as one of the physical methods of 86.8–99 % yield for dye removal from industrial effluents is considered as simple and effective [9]. It is thought to be highly economical due to the ease of handling, as well as the possibility of reusing the adsorbents in subsequent sorption–desorption cycles. It has been estimated that the average cost of wastewater treatment by adsorption is US$ 5.0–200/m^3, while other technologies are in the range of US$10.0–450/$m^3$ [10]. It is therefore particularly important to obtain new adsorbents, especially those containing biocomponents in their composition, making them more biodegradable and low-cost materials [11,12]. It is also important to use biocomponents that are post-process wastes in the synthesis of new adsorptive materials. In recent years, adsorbents containing such biodegradable additives as lignin [13], cellulose [14,15], eugenol [16,17], or starch [18] have attracted great interest in wastewater treatment technologies.

Starch belongs to the group of polysaccharides of plant origin. It is composed of glucose mers linked by α-glycosidic bonds and acts as an energy store in plants. Starch is a very interesting biopolymer, the possibilities for its use in sorption processes being created by its very interesting structure resulting from the presence of hydroxyl groups. The undoubted advantages of using starch are its very wide availability, low price, and hydrophilic nature. What limits the use of starch is its poor mechanical resistance and partial solubility in hot water. The use of starch as an additive in the synthesis of polymeric microspheres can significantly improve the aforementioned properties and broaden the range of potential applications of this interesting biopolymer considerably [19,20]. Various techniques of starch modification by physical (annealing, high hydrostatic pressure, or ultrasonic treatment), chemical (cross-linking, grafting, esterification or etherification), and enzymatic (debranching enzymes such as isoamylase and pullulanase) methods make it possible to develop new innovative adsorbent materials for the removal of dyes and other toxic compounds from wastewaters [21–27]. Such modifications make it feasible to obtain adsorbents with a much higher sorption capacity compared to native starch and greater mechanical strength, which is extremely important for wastewater treatment in column operation systems [28]. In addition, the biodegradability of such adsorptive materials is enhanced due to the presence of the biocomponent which makes them more inexpensive sorbents [29,30] and replaces traditional petrochemical and non-biodegradable materials [31–34]. From a technological point of view, the newly synthesized materials must be characterized by mechanical, thermal, and chemical resistance, as well as a spherical shape, which reduces flow resistance in the column system [32]. Adsorbents containing starch have been applied to remove dyes such as Crystal Violet [35], Methylene Orange and Methylene Blue [34], Congo Red and Rhodamine B [34,35], Malachite Green [36], Acid Black 234 [37], Direct Red 80 [38], Direct Red 23 and Acid Blue 92 [39], Amaranth, Tartrazine, Sunset Yellow and Eosin Yellow [40], etc.

This study aimed to synthesize new innovative polymer microspheres based on poly(ethylene glycol dimethacrylate-co-vinyl acetate) containing mechanochemical modified starch with thiourea and potassium dihydrogen phosphate and to evaluate the adsorption potential against toxic dye of cationic type. To our knowledge, this is the first research on the feasibility of using such adsorbents for the removal of C. I. Basic Yellow 2. The suspension polymerization method was used to obtain the materials in spherical form. The reaction was carried out in an aqueous medium using polyvinyl alcohol as a suspension stabilizer. A

Table 1
Experimental parameters of synthesis.

Sample No	EDGMA (g)	VA (g)	St (g)	St/T (g)	St/P (g)	AIBN (g)
1	10.00	4.30	3.00	–	–	0.15
2	10.00	4.30	–	3.00	–	0.15
3	10.00	4.30	–	–	3.00	0.15
4	10.00	4.30	–	–	–	0.15

where: EGDMA – ethylene glycol dimethacrylate, VA – vinyl acetate, St – unmodified starch, St/T – thiourea (T) modified starch, St/P – KH_2PO_4 (P) modified starch, AIBN – α,α'-azobis(isobutyronitrile).

reference material without any modification of starch was also synthesized and investigated. Adsorptive kinetic and equilibrium parameters were calculated based on popular models. The uptake of BY2 was studied in the presence of additives such as electrolytes and cationic surfactants. Regeneration possibilities of obtained adsorbents were investigated, too.

2. Materials and methods

2.1. Chemicals and eluents

Ethylene glycol dimethacrylate (EGDMA), vinyl acetate (VA), poly (vinyl alcohol) (PVA), α,α'-azobis(isobutyronitrile) (AIBN), and cationic surfactant cetyltrimethylammonium bromide (CTAB) were obtained from Sigma-Aldrich (Germany). Starch (St) soluble and $CaCl_2$ were purchased from Chempur (Poland). Benzyl alcohol, acetone, hydrochloric acid, sodium chloride, sulphate and hydroxide, tetrahydrofurane (THF), dichloromethane (CH_2Cl_2), methanol (MeOH), potassium dihydrogen phosphate(V) (P) as well as thiourea (T) were obtained from Avantor Performance Materials Poland S.A. (Poland). C.I. Basic Yellow 2 (BY2) dye used as an adsorbate was purchased from the company Sigma-Aldrich (Germany) and its characteristic is presented in Fig. 1 and **Fig. S1** (**Supplementary materials**).

2.2. Modification of starch

Starch modification was carried out using a mechanochemical method [41–43]. 15.00 g of soluble starch was mixed and highly grated in a mash pot with 7.60 g (0.10 mol) of thiourea, or 7.00 g (0.075 mol) of potassium dihydrogen phosphate(V) for 45 min. The grated mixture was then dried-heated in a chamber at 90–95 °C for 10 h, to constant weight. Cyclically, the grinding – mixing of the ingredients was repeated every two hours.

2.3. Preparation of microspheres

The synthesis of microspheres was performed in the aqueous medium, using the suspension-polymerization method [44–47]. 150 mL of redistilled water, 1.00 g of poly(vinyl alcohol), and 1.20 g $CaCl_2$ were stirred for 0.5 h at 80 °C in a three-necked flask fitted with a thermometer, a water condenser, and a mechanical stirrer. 3.00 g of starch of different types (Table 1) were previously dissolved in 15 mL of benzyl alcohol (2 h at 60 °C). Then, the solution containing: 10.00 g of the ethylene glycol dimethacrylate and 4.30 g of vinyl acetate in molar mass 1:1, 1 % wt. of initiator α,α'-azobis(isobutyronitrile). Then the mixture of benzyl alcohol with starch was added to the aqueous medium. Copolymerization was completed for 10 h at 80–85 °C. The obtained microspheres were washed with distilled water (2000 mL) and acetone (200 mL). The chemical structures of monomers are presented in Fig. 2. Adsorbents were dried at 80 °C to a constant weight.

2.4. Measurements

The Fourier transform infrared (FT-IR) spectra were recorded with a Bruker Tensor 27 FTIR spectrometer (Germany) using the attenuated total reflectance (ATR) technique. The samples were thin films. All spectra were obtained at room temperature after averaging 32 scans between 600 and 4000 cm^{-1} with a resolution of 4 cm^{-1} in the absorbance mode.

The differential scanning calorimetry (DSC) method was performed using a Netzsch DSC 204 calorimeter (Germany) operated in the dynamic mode. DSC measurements were made by applying aluminum pans with pierced lids and a sample mass of ~ 5–10 mg under a nitrogen atmosphere (30 mL/min). Dynamic scans were performed at a heating rate of 10 °C/min in the temperature range of −20 to 600 °C. The parameters such as the range of decomposition temperatures (T_{onset}, T_{offset}) and maximum decomposition temperature (T_d) were determined.

The porous structures of the copolymers were characterized by the N_2 adsorption method at −196 °C (ASAP 2405 adsorption analyzer, Micrometrics Inc., USA). Before the analysis, the copolymers were degassed at 120 °C for 2 h. The specific surface area was calculated according to the Brunauer-Emmett-Teller (BET) method with the assumption that the area occupied by a single nitrogen molecule is 16.2 $Å^2$. The pore volumes and pore size distributions were determined by the

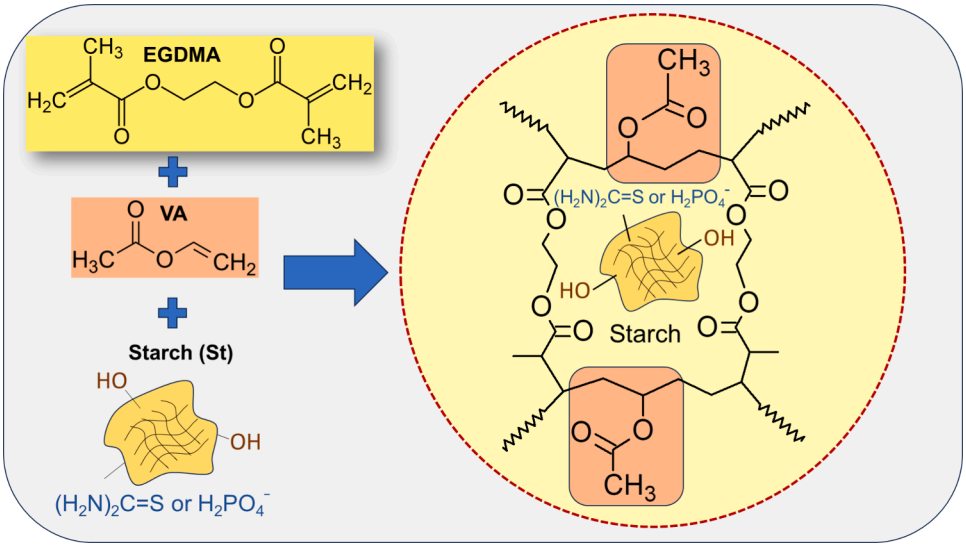

Fig. 2. Chemical structures of monomers used for the polymerization reaction.

Barrett-Joyner-Halenda (BJH) method.

The scanning electron microscope (SEM) Quanta 3D FEG with the acceleration voltage 20 kV coupled with energy dispersive X-ray spectroscopy method (EDX) (FEI, US) was applied for visualization of morphology and microstructure of starch-modified adsorbents as well as their composition.

The chemical compositions of adsorbents were analyzed by the X-ray photoelectron spectroscopy (XPS) method. A multi-chamber ultra-high vacuum XPS UHV apparatus and monochromatic X-rays (Gammadata Scienta MX-650 source, Kα-Al anode; Prevac, USA) were used for this purpose.

The surface charge properties of the starch-based adsorbents were investigated by determining the pH at zero charge point (pH_{pzc}). In this method, 0.01 M KCl solutions were prepared of different initial pH (pH_0) values (2, 4, 6, 8, 10, and 12) by addition of 0.1 M NaOH or HCl using pH-meter CPC-411 (Elmetron, Poland). Next, 0.05 g of the adsorbents were equilibrated in a laboratory shaker Elpin + 358S (Elpin, Lubawa, Poland) for 24 h with 20 mL of the solutions of specific pH_0. Then, the final pH (pH_f) of the solutions was measured. The pH_{pzc} values of synthesized microspheres were obtained by plotting ΔpH ($\Delta pH = pH_0 - pH_f$) versus pH_0.

The particle size distribution of the adsorbents under study was determined by the laser light diffraction (LDS) method using a laser particle size analyzer Mastersizer 2000 (Malvern Instruments, U.K). Before testing, the measuring cell was filled with distilled water, the pump was started and the relevant measurement parameters, such as RI, sample optical parameters, radiation absorption, and pump speed, were set. The test sample was then gradually added to the measuring cell containing the redistilled water, taking care not to exceed the obscuration limit displayed on the monitor in the instrument software. For each sample, 10 measurement cycles were performed, from which the arithmetic mean and standard deviation were calculated for the three parameters: d(0.1), d(0.5) and d(0.9).

0.1 g of microspheres were placed in a glass tube with a sinter and their volume was measured. A suitable organic solvent or water was then poured in and the increase in volume of the adsorbents after swelling was monitored. The swellability coefficients (B) were determined according to Eq. (1)

$$B = \frac{V_s - V_d}{V_d} 100\% \quad (1)$$

where: V_s – the volume of the polymeric adsorbent modified with starch after swelling (mL), V_d – the volume of the dry polymeric adsorbent modified with starch (mL).

2.5. Adsorption and desorption tests

Batch adsorption method was used to determine the equilibrium and kinetic adsorption parameters. 0.05 g of the adsorbent was weighed out into Erlenmajer flasks, then 20 mL of BY2 solution at the specified initial concentration ranging from 1 to 100 mg/L was poured in. According to preliminary studies, maximum dye removal with bioadsorbents was recorded at pH=8.3 (pH-meter CPC-411, Elmetron, Poland), **Fig. S2, Supplementary materials**). The flasks were placed in a mechanical shaker Elpin + 358S (Elpin, Lubawa, Poland) with a constant oscillation amplitude (A=8, 170 cycle/min), and the contents were shaken for 1 min up to 24 h at 298 K. Equilibrium studies were conducted as a function of initial dye concentration (1–25 mg/L, pH=8.3) at 24 h of shaking time. Kinetic experiments were carried out as a function of time (t), from 1 min to 60 min using BY2 solution of the initial concentration 10 mg/L at pH=8.3. The impact of electrolyte (5–15 g/L Na_2SO_4) and cationic surfactant (0.1–0.5 g/L CTAB) on BY2 (10 mg/L) removal efficiency was investigated at phase contact time 15 min. Temperature effect on BY2 (100 mg/L, pH=8.3) sorption was investigated at 298, 308, 318, and 328 K during 240 min of phase contact time.

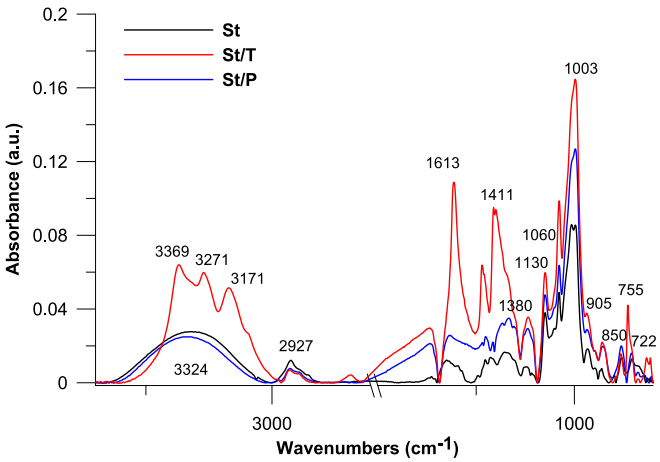

Fig. 3. ATR/FT-IR spectra of starch before and after modifications.

The solution was filtered and the dye concentration after sorption was determined by the spectrophotometric method against blank as reference using a Cary 60 UV–vis spectrophotometer (Agilent Technologies, Santa Clara, CA, USA) at 431 nm.

The amounts of BY2 uptaken by adsorbents containing modified starch after specific time (q_t) and the adsorption capacities (q_e) were calculated based on the following Equations:

$$q_t = \frac{(C_0 - C_t)}{m} V \quad (2)$$

$$q_e = \frac{(C_0 - C_e)}{m} V \quad (3)$$

where: C_0, C_t, C_e – the dye concentration initially, after specific sorption time and at equilibrium, respectively (mg/L), V – the volume of adsorbate (L), m – the adsorbent mass (g).

Desorption experiments were performed by the batch method involving two steps. The first stage was the sorption of BY2 on polymeric microspheres containing modified starch under the following experimental conditions: initial dye concentration – 10 mg/L BY2, volume of BY2 solution – 20 mL, adsorbent mass – 0.05 g, sorption time – 120 min, shaking parameters – A=8 and 180 cycle/min. The second stage consisted of the removal of BY2 from the adsorbent phase using eluents such as 1 M HCl, 1 M NaCl, 1 M NaOH, 50 % v/v MeOH, 1 M HCl + 50 % v/v MeOH, 1 M NaCl + 50 % v/v MeOH, 1 M NaOH+50 % v/v MeOH. The conditions were as follows: volume of eluent solution – 20 mL, adsorbent mass with loaded BY2 – 0.05 g, desorption time – 120 min, shaking parameters – A=8, and 180 cycle/min. After solution separation, the BY2 dye content was determined spectrophotometrically and the desorption (D) efficiency was calculated from Equation (4):

$$D = \frac{m_{des}}{m_{ads}} 100\% \quad (4)$$

where: m_{des} – the mass of desorbed BY2 (mg), m_{ads} – the mass of adsorbed BY2 (mg).

The batch adsorption/desorption experiments were performed in triplicates and the mean value of the results was used for data evaluation (the reproducibility ± 5 %).

3. Results and discussion

3.1. Characteristics of polymeric microspheres containing modified starch

In the first stage of work, the modification of the original starch took place. To confirm the modification the ATR/FT-IR spectra of the obtained new starch materials (Fig. 3) were performed. On the spectra of

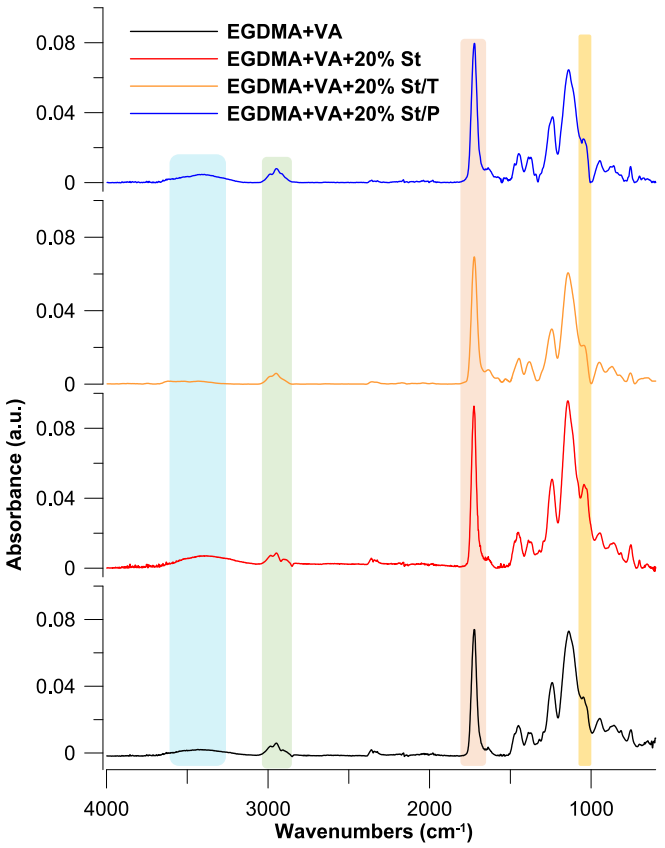

Fig. 4. ATR/FT-IR spectra of polymeric microspheres with modified starch.

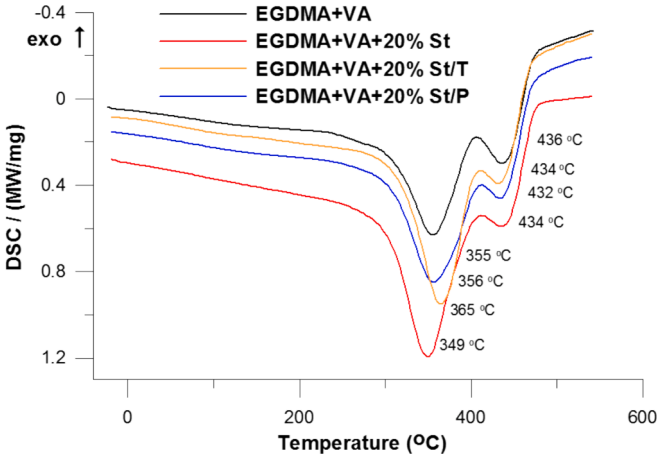

Fig. 5. DSC curves of the obtained microspheres.

pure starch, the wide absorption band around 3200–3500 cm^{-1} is assigned to the stretching vibrations of hydroxyl groups (O–H). The signal around 2920 cm^{-1} is attributed to stretching vibrations in the C–H aliphatic. The signals: 1130, 1115, 1105, and 1003 cm^{-1} correspond to –OH groups. In turn, the 905, 850, and 722 cm^{-1} vibrations are assigned to the pyrazone system. In the case of starch modification with KH_2PO_4, the signal 1275 cm^{-1} corresponds probably to P=O groups, and the signals 1060 and 970 (together with C-O) P-O vibrations. Clear changes can be observed on the spectrum of thiourea-modified starch. The vibrations of NH groups at 3369, 3271, and 3171 cm^{-1} overlaid with OH groups are marked on the spectra. Additionally, the signal at 1380 cm^{-1} corresponds to amide groups (S=C-NH). The strong signal at 1613 cm^{-1} can be attributed to $–NH_2$ groups.

Table 2
Parameters of the porous structures of the studied microspheres.

Adsorbent	Specific surface area, S_{BET} (m^2/g)	Pore volume, V_{TOT} (cm^3/g)	Average pore diameter, W (nm)	The most probable pore diameter (nm)
EGDMA+VA	207	0.231	5.35	3.80
EGDMA+VA+20 % St	235	0.304	5.84	3.90
EGDMA+VA+20 % St/T	176	0.224	5.09	2.50
EGDMA+VA+20 % St/P	190	0.309	6.51	3.8/8.0

The ATR/FT-IR spectra of the obtained microspheres with starch are presented in Fig. 4. The obtained curves for all materials possess similar courses strongly connected with groups presented in main monomers: EGDMA and VA. By analyzing the course of the curves, we can conclude that mainly, an increase in the intensity of bands originating from oxygen-containing groups i.e. O–H hydroxyl groups (about 3400 cm^{-1}) and –C-OH and C-O-C groups (about 1050 cm^{-1}) is observed. The most important bands are marked on the spectra. The wide absorption band around 3300–3450 cm^{-1} is assigned to the stretching vibrations of hydroxyl groups and it slightly increases with the amount of non-modified and St/P-modified starch in polymeric microspheres. The signal around 2980–2940 cm^{-1} is qualified to stretching vibrations in C–H aliphatic. The characteristic sharp signal around 1720 cm^{-1} is assigned to C=O stretching vibrations mainly from EGDMA.

The thermal characteristics of the microspheres were investigated by the DSC method. The DSC curves with marked temperatures are presented in Fig. 5. On the curves two endothermic effects (349–356 and 432–436 °C) associated with the thermal degradation process (T_d) of the samples are visible. The first endothermic effect corresponds to the degradation of vinyl acetate and starch fragments. In contrast, the second endothermic effect is responsible for the degradation of crosslinked fragments of polymeric chains. No exothermic effect at about 170–200 °C associated with the process of crosslinking is noticeable, which indicates a complete conversion of the double bonds. With the addition of modified starch, especially in the case of thiourea, decomposition takes place at a slightly higher temperature (c.a. 10 °C) in comparison to parent EGDMA+VA materials. Analysis of the obtained results leads to the conclusion that adding modified starch does not reduce the thermal resistance of microspheres. In the case of unmodified starch, the reduction in maximum decomposition temperature is only 6 °C.

The characteristic parameters of the porous structures of the studied microspheres are presented in Table 2. The specific surface areas (S_{BET})

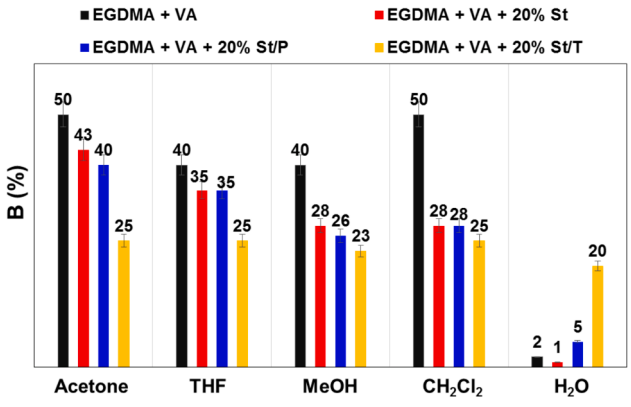

Fig. 6. Swellability coefficients for obtained adsorbents.

(a) EGDMA + VA

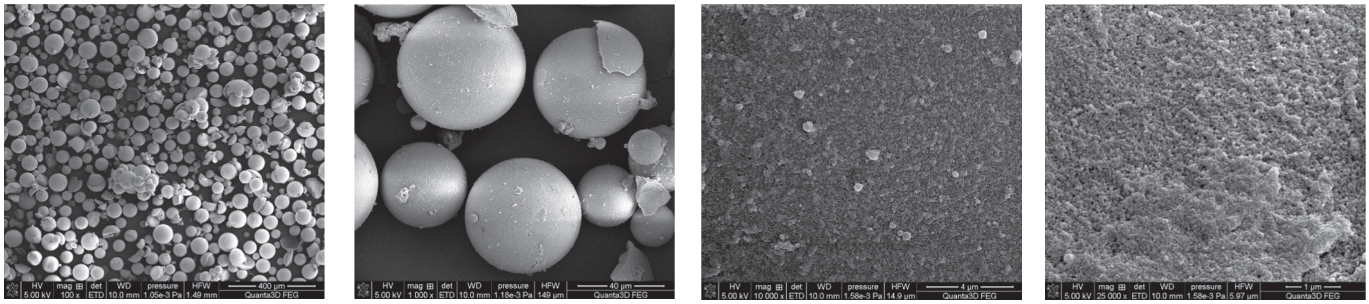

mag. 100× mag. 1000× mag. 10 000× mag. 25 000×

Element	CK	OK	AlK	SiK	Total
Wt (%)	67.96	31.97	0.04	0.04	100
At (%)	73.87	26.09	0.02	0.02	100

(b) EGDMA + VA + 20% St

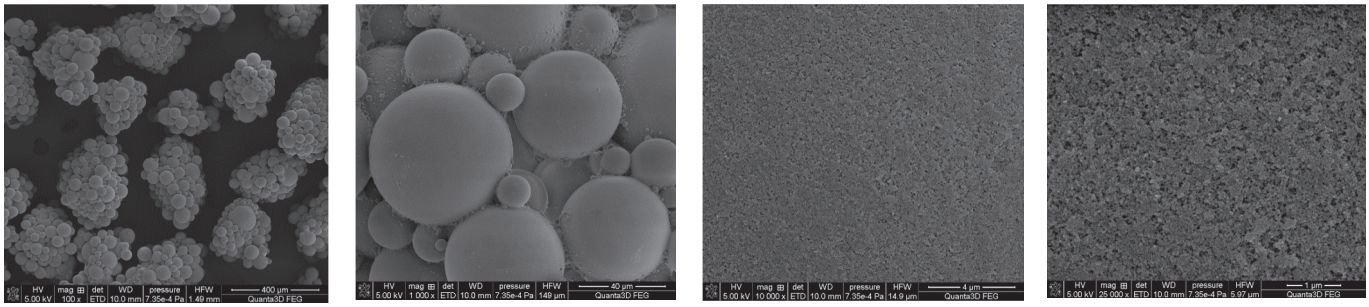

mag. 100× mag. 1000× mag. 10 000× mag. 25 000×

Element	CK	OK	AlK	SiK	Total
Wt (%)	70.08	29.85	0.04	0.03	100
At (%)	75.75	24.22	0.02	0.01	100

(c) EGDMA + VA + 20% St/P

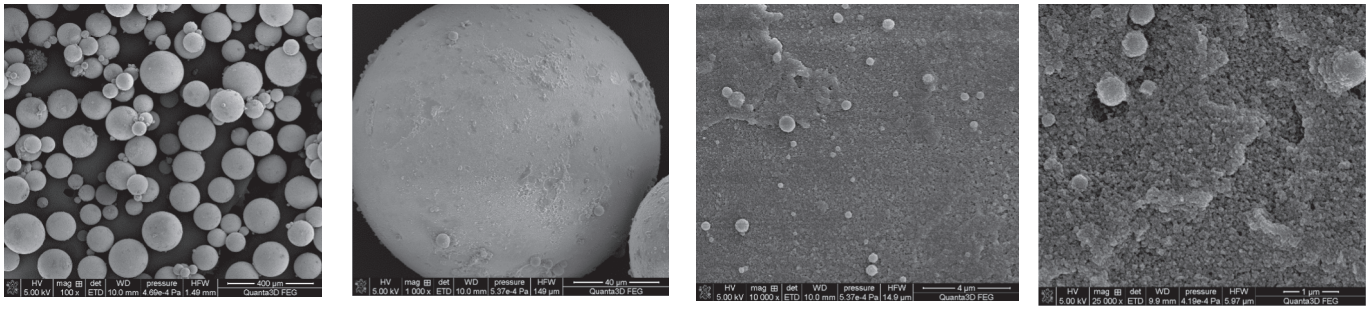

mag. 100× mag. 1000× mag. 10 000× mag. 25 000×

Element	CK	OK	AlK	SiK	PK	Total
Wt (%)	74.59	25.18	0.06	0.09	0.08	100
At (%)	79.72	20.18	0.03	0.04	0.03	100

(d) EGDMA + VA + 20% St/T

Fig. 7. Starch-modified microspheres visualization and composition by the SEM-EDX analysis.

and total pore volumes (V_{tot}) are in the ranges of 176 to 235 m^2/g and 0.224 to 0.309 cm^3/g, respectively. These materials are mesoporous the average pore diameter (W) is approximately 5 nm. The largest specific areas and pore volumes are observed for the microspheres EGDMA+VA+20 % St. With adding the modified starch, the decreases in S_{BET}, V_{TOT}, as well as W, are noticeable. This observation is probably

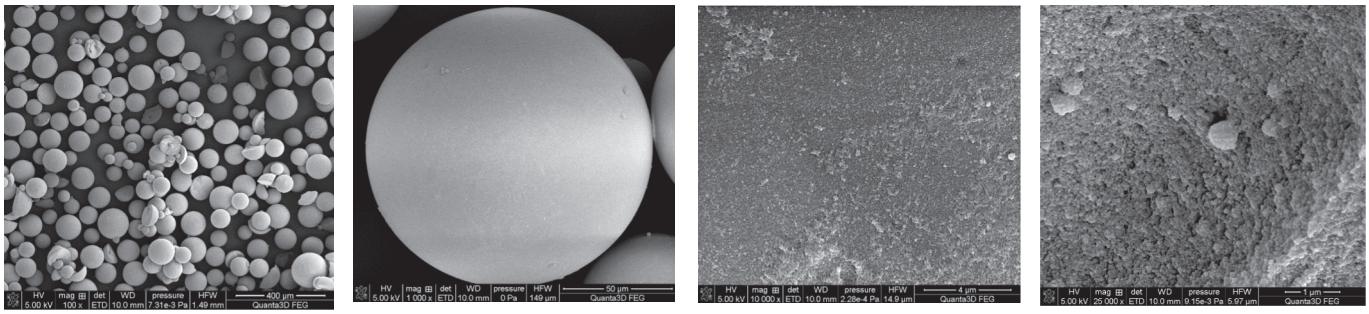

mag. 100× mag. 1000× mag. 10 000× mag. 25 000×

Element	CK	OK	AlK	SiK	SK	Total
Wt (%)	72.62	27.21	0.04	0.05	0.07	100
At (%)	77.99	21.94	0.02	0.02	0.03	100

(e) EGDMA + VA + 20% St/T after BY2 sorption

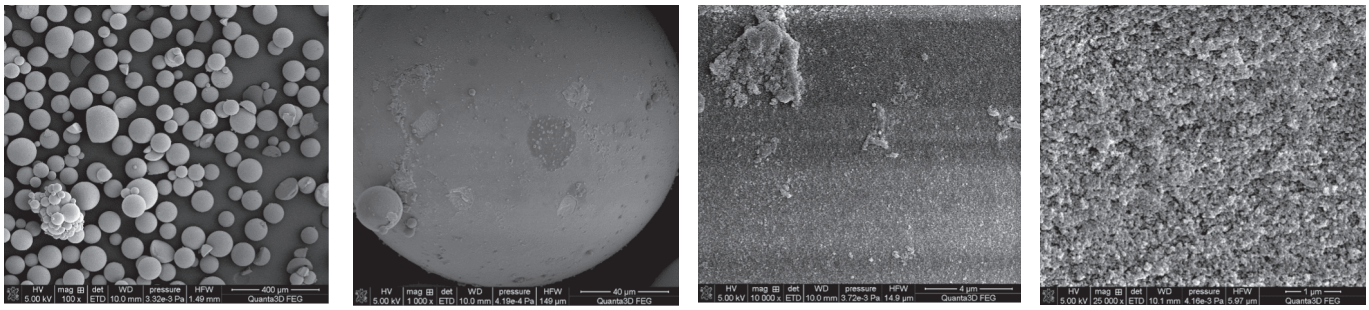

mag. 100× mag. 1000× mag. 10 000× mag. 25 000×

Element	CK	NK	OK	AlK	SiK	SK	Total
Wt (%)	73.99	1.08	24.74	0.06	0.04	0.08	100
At (%)	79.08	0.99	19.85	0.03	0.02	0.03	100

Fig. 7. (*continued*).

connected with the blocking of pores by partially bound molecules of modified starch. Worth noting is that microspheres EGDMA+VA+20 % St/P possess two maxima in 3.8 and 8.0 nm for the most probable pore diameter compared to other materials.

The results of the swelling studies for the synthesized microspheres are presented in Fig. 6. The swellability coefficients (B) were indicated using typical solvents (acetone, methanol, dichloromethane, and water). Among the studied materials, the highest tendency to swell is detected for the unmodified (pristine) microspheres (B=50 %). All studied materials possess a tendency to swell in organic solvents. The smallest values of B were obtained for the water, only EGDMA+VA+20 % St/T microspheres, 20 % was achieved. With the addition of specially modified starch to the structure of microspheres the tendency to swell decreases. The chemical nature of microspheres changes and this affects the tendency to swell.

The surface morphology of adsorbents before and after BY2 sorption was characterized using SEM microscopy. The SEM images were recorded with the magnification of 100, 1000, 10 000, and 25 000 × and are presented in Fig. 7. They show that all obtained adsorbents are spherically shaped beads and their irregular surface structure possesses pores. An increase in the particle diameter of the adsorbents of about 50 % was observed with the addition of starch, both unmodified and modified. A particular tendency towards the aggregation of microspheres can be seen in the case of the EGDMA+VA+20 % St. The aggregates resemble clusters of grapes. Micro clusters of starch modifiers can be seen on the surface of the particles. The quantitative composition of the EGDMA+VA, EGDMA+VA+20 % St, EGDMA+VA+20 % St/T, and EGDMA+VA+20 % St/P is also presented in Fig. 7. The contents (in weight %) of carbon, oxygen, aluminium, silicon, sulphur and phosphorous are in equaled to 67.96–74.59 %, 25.18–31.97 %, 0.04–0.06 %, 0.03–0.09 %, ≈0.07 %, and ≈0.08 % respectively. This demonstrates the effective embedding of modifiers.

The XPS method was used to assess the atomic concentration (C_{at}, %) values of the elements in the surface layer of the adsorbents. It should be emphasized that this is a method that does not allow the estimation of C_{at} in the whole volume of the sample and its results may be slightly different from those obtained by the EDX method. Fig. 8 presents the wide-scan XPS spectra of obtained pristine adsorptive materials and after starch modification. Table 3 presents the band's identification of the EGDMA+VA, EGDMA+VA+20 % St, EGDMA+VA+20 % St/T, and EGDMA+VA+20 % St/P and indicates the effective incorporation of the modified starch into the polymer matrix. The studied sorbents were characterized by bands recording of the C 1 s, O 1 s, Na 1 s, Si 2p for EGDMA+VA, C 1 s, O 1 s, Si 2p for EGDMA+VA+20 % St, C 1 s, O 1 s, Si 2p, P 2p for EGDMA+VA+20 % St/P as well as C 1 s, O 1 s, Si 2p, N 1 s, S 2p 3/2 and S 2p 1/2 for EGDMA+VA+20 % St/T (Fig. 8). The electron configurations of carbon and oxygen into pristine material and after modified starch addition were studied concerning possible interactions between modifiers and matrix. The C1s signal in EGDMA+VA+20 % St was decomposed into four peaks located at 284.8 eV for C–C/C–H groups, at 286.3 eV for C-OH/C-O-C groups, at 287.6 eV for C=O group and 288.7 eV for COOH group. Next, the O1s signal was decomposed into three peaks, the binding energy peaks located at 532 eV, 533.3 eV, and 535 eV can be assigned to O=C, C–O–C/C-OH as well as water,

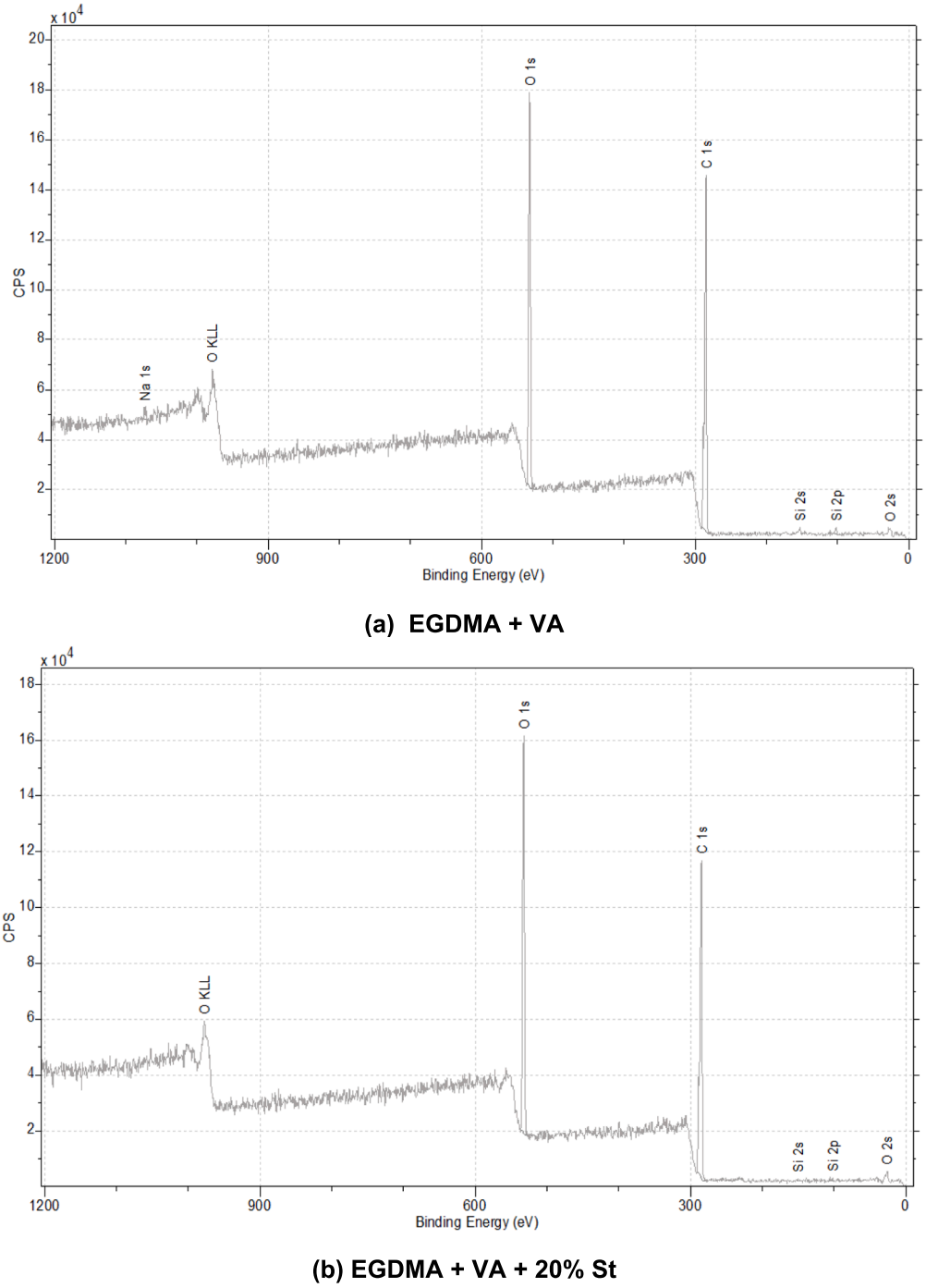

Fig. 8. The wide-scan XPS spectra (a-d) of synthesized adsorbents and high-resolution spectra of EGDMA+VA+20 % St/T (e).

respectively. In the case of EGDMA+VA+20 % St/T adsorbent there are observed additional peaks attributed to C=S, $-NH_2$, and sulphur as presented in Fig. 8**(e)**.

The particle size distribution analysis provided information on the dispersion, grain morphology, and agglomeration tendency of the obtained adsorbents modified with starch. The results are presented in Table 4. The size of EGDMA+VA polymer beads is in the range 59.98–199.46 μm. An increase in bead size is observed after the addition of starch as a modifier. It was also shown that the synthesized biopolymers were characterized by heterodispersity. In the case of EGDMA+VA+20 % St/T and EGDMA+VA+20 % St/P, 10 % of adsorbent beads are smaller than 76.9 μm and 113.06 μm, 50 % is smaller than 107.04 μm and 163.97 μm, and 90 % is smaller than 145 μm and 223.21 μm, respectively.

Determination of the pH_{pzc} value of the biosorbents provides insight into the possible ionization and interactions of functional groups with the dye in solution and contributes to the understanding of the likely sorption mechanism. Fig. 9 presents the surface charge of synthesized materials as a function of pH. The pH_{pzc} of the EGDMA+VA, EGDMA+VA+20 % St, EGDMA+VA+20 % St/T, and EGDMA+VA+20 % St/P were found to be 7.05, 6.30, 6.80 and 6.88, respectively. When the pH of adsorbate solution is higher than pH_{pzc}, the favorable adsorption of positive ions is observed, while for pH lower than pH_{pzc} biosorption of negative ions occurs. Under experimental conditions

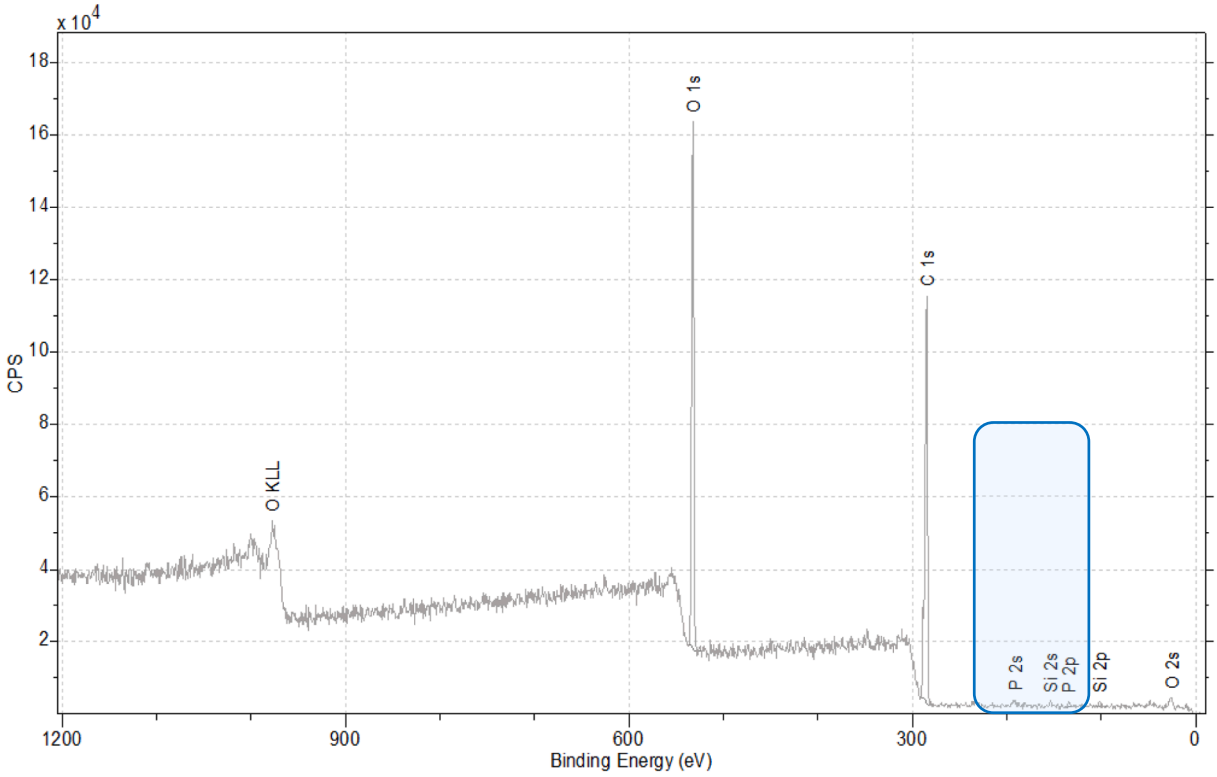

(c) EGDMA + VA + 20% St/P

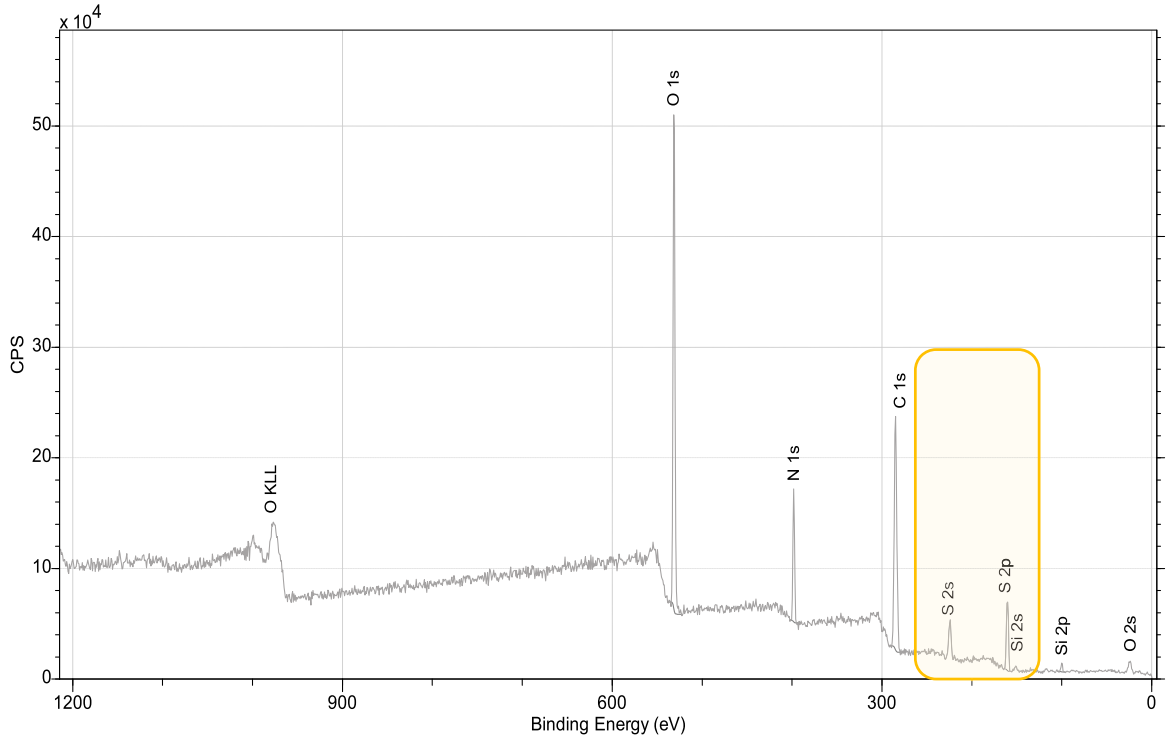

(d) EGDMA + VA + 20% St/T

Fig. 8. (*continued*).

negatively charged surface of prepared adsorbents interacts with BY2 dye cations. According to Kongseng et al. [48], the pH_{pzc} of the cassava starch (CS) and VA composite was 6.5 during methylene blue adsorption. pH_{pzc} of hydrogels based on starch and carboxymethyl cellulose (CMC) crosslinked with sodium trimetaphosphate was in the range of 4.02–5.5 [49]. Starch-based nanocomposites applied for

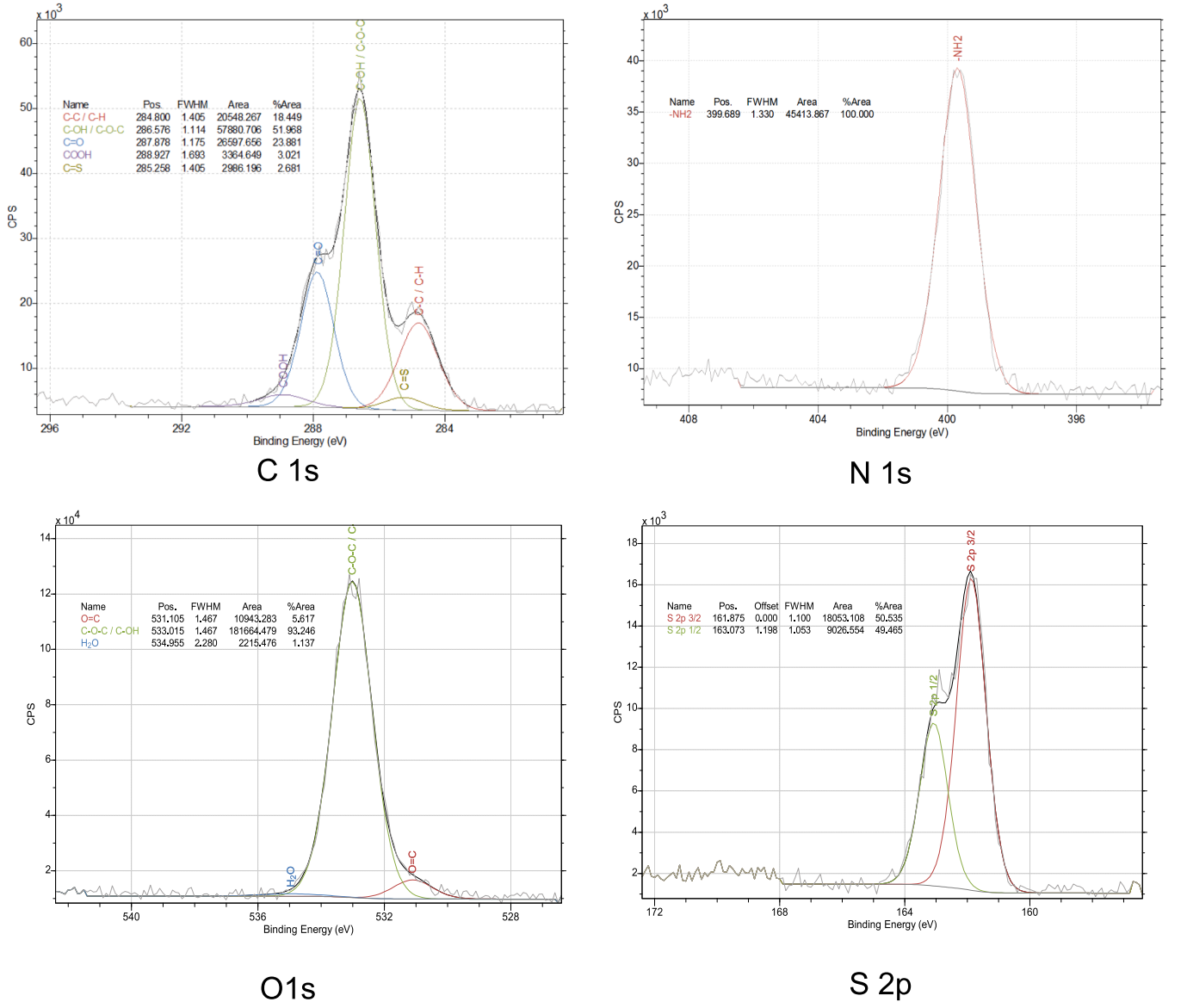

Fig. 8. (*continued*).

methylene blue removal have a pH_{pzc} of 4–5 [38].

3.2. Adsorption test

3.2.1. Equilibrium parameters

To determine the adsorption capacities, i.e. the correlation between the initial BY2 adsorbate concentration and its equilibrium concentration using starch-containing adsorbents, the experimental data were fitted to Langmuir (Equation 5), Freundlich (Equation 6), Temkin (Equation 7) and Dubinin-Raduschkevich (Equation 8) isotherm models. The equilibrium parameters were calculated using linear forms of the isotherm models:

$$\frac{C_e}{q_e} = \frac{1}{Q_0 k_L} + \frac{C_e}{Q_0} \tag{5}$$

$$logq_e = logk_F + \frac{1}{n} logC_e \tag{6}$$

$$q_e = \left(\frac{RT}{b_T}\right) lnA + \left(\frac{RT}{b_T}\right) lnC_e \tag{7}$$

$$lnq_e = lnq_m - k_{DR}\varepsilon^2 \tag{8}$$

where: q_e – the adsorption capacity (mg/g), C_e – the equilibrium concentration of BY2 in solutions (mg/L), Q_0 – the monolayer adsorption capacity (mg/g), k_L – the Langmuir constant (relating to the free energy of adsorption) (L/mg), k_F ($mg^{1-1/n}$ $L^{1/n}$/g) and 1/n – the Freundlich constants regarding to adsorption capacity and the surface heterogeneity, respectively, R – the gas constant (8.314 J/mol K), T – the temperature (K), A (L/mg) and b_T (J/mol g/mg) – the Temkin constants, q_m (mg/g) – the maximum adsorption capacity, k_{DR} (mol^2/J^2) – the constant concerning the adsorption energy, ε (J/mol) – the adsorption potential [50].

The isotherm parameters were calculated by applying linear regression and using the following plots: C_e/q_e vs C_e, log q_e vs log C_e, q_e vs ln C_e, and ln q_e vs ε^2 [51]. The values of determination coefficient

Table 3
Results of qualitative and quantitative analysis for starch-modified adsorbents using XPS method.

Adsorbent	Level	Position (eV)	C_{at} (%)	Standard deviation (%)
EGDMA+VA	C 1 s	284.8	73.5	0.073
	O 1 s	533.1	25.1	0.065
	Na 1 s	1071.6	0.2	0.017
	Si 2p	101.8	1.2	0.043
EGDMA+VA+20 % St	C 1 s	284.8	73.5	0.099
	O 1 s	532.3	25.8	0.092
	Si 2p	105.6	0.7	0.052
EGDMA+VA+20 % St/P	C 1 s	284.8	71.5	0.121
	O 1 s	532.3	26.9	0.088
	Si 2p	101.1	0.8	0.108
	P 2p	134.1	0.8	0.061
EGDMA+VA+20 % St/T	C 1 s	284.8	52.0	0.082
	N 1 s	398.1	10.5	0.068
	S 2p	160.3	7.3	0.027
	O 1 s	531.6	28.7	0.061
	Si 2p	100.3	1.5	0.035

Table 4
Particle size distribution of the synthesized adsorbents.

Adsorbent	d(0.1) (μm)	d(0.5) (μm)	d(0.9) (μm)
EGDMA+VA	59.98	90.56	199.46
EGDMA+VA+20 % St	102.87	207.65	331.79
EGDMA+VA+20 % St/T	76.90	107.04	145.00
EGDMA+VA+20 % St/P	113.06	163.97	223.21

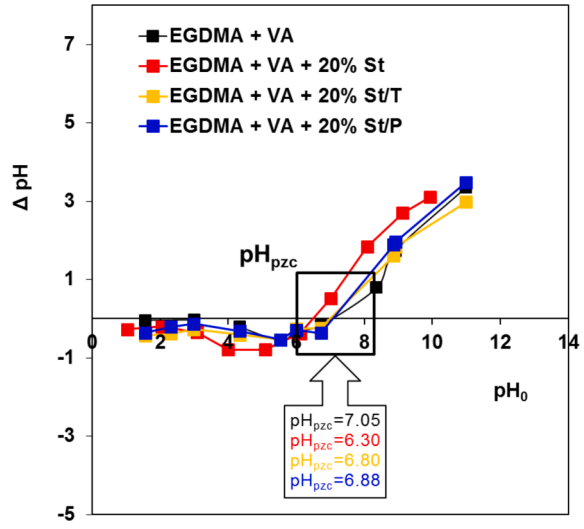

Fig. 9. Determination of pH_{pzc} of synthesized adsorbents.

(R^2), chi-square (χ^2), and residual sum of squares error (SSE) were calculated and taken into account to establish the best-fitting model for adsorption data [50–53].

Table 5 includes calculated isotherm parameters for the investigated adsorption systems and Fig. 10 displays the fitting of the isotherm models to equilibrium sorption data of BY2 on starch-modified adsorbents.

Analysis of the compiled parameters and the distribution of experimental points with fitting of isotherm models allows us to conclude that the most suitable model for describing the adsorption of BY2 on EGDMA+VA, EGDMA+VA+20 % St, EGDMA+VA+20 % St/T and EGDMA+VA+20 % St/P is the Freundlich model (R^2 = 0.974–0.997, SSE=0.48–1.22, χ^2 = 0.09–0.29). The Freundlich model defines multilayer adsorption on heterogeneous surfaces. The k_F values reflected the intensity of adsorption and were found to be in the range of 5.62–6.56 $mg^{1-1/n}\,L^{1/n}$. The highest value of k_F was determined for BY2 adsorption on the EGDMA+VA+20 % St/T. The obtained results allowed us to determine the applicability series of starch-modified polymeric adsorbents towards BY2 as follows: EGDMA+VA+20 % St/T>EGDMA+VA+20 % St > EGDMA+VA>EGDMA+VA+20 % St/P. The parameters 1/n were smaller than 1 which points to favorable adsorption. The applicability of the Freundlich isotherm model for the description of BY2 adsorption is presented in Table 6 [53–60] and was confirmed for the carbon/silica composite [55], hybrid microspheres with co-participated lignin [56], polystyrene-based resins with chloride groups [57] or diphenylvinylphoshine oxide based resins [58]. **Figure S3** (**Supplementary materials**) presents proposed interactions between BY2 dye and polymeric microspheres containing modified starch, which may include: a dimethylamine group and hydrogen of the –OH group of the starch or modifier $H_2PO_4^-$, a dimethylamine group and hydrogen of the amide in thiourea, a secondary ammonium salt in BY2 and oxygen from an ester group, and a phosphate group, secondary ammonium salt in BY2 and oxygen from C-O-C ester group or –OH group of starch, secondary ammonium salt in BY2 and sulphur from thiourea, a dye aromatic system and an aliphatic ethylene chain $–CH_2-CH_2-$ from vinyl acetate, ethylene glycol (EGDMA) or polymethacrylate.

According to the Langmuir isotherm model, the formation of monolayer coverage of BY2 dye molecules on the surface of starch-modified adsorbents should be occur. The monolayer adsorption capacity of EGDMA+VA+20 % St/T was the highest one and equaled 18.87 mg/g. However, the R^2 values for this model were smaller than for the Freundlich model, while the SSE and χ^2 values were larger than for the Freundlich model, which argues in favor of using the latter to describe the experimental data.

It can be stated from the Temkin isotherm model that the BY2 adsorption heat in the surface layer decreases not logarithmically but linearly. The A and b_T constant values from the Temkin equation are listed in Table 5. The R^2, SSE, and χ^2 values confirm that the model is not applicable from the description of experimental data. Furthermore, for very low adsorbate concentrations, the calculated sorption capacities are negative, which does not make physical sense.

The Dubinin-Raduschkevich isotherm model gives an idea about the sorption process type, whether this is a physical or chemical reaction.

The mean sorption energy E, calculated from the Dubinin-Raduschkevich isotherm model as $E = \frac{1}{\sqrt{2k_{DR}}}$, can give an information of the type of sorption process, whether it is a physical or chemical reaction. If E values are smaller than 8 kJ/mol, physical adsorption occurs, otherwise chemical adsorption predominates. In the systems studied, the E values ranged from 3.60 to 4.89 kJ/mol, indicating the physical nature of the binding of BY2 cations by the starch-modified polymeric microspheres. The calculated sorption capacities q_m in the range 5.91–6.75 mg/g as well as the constant connected with the adsorption mean free energy ($2.1 \times 10^{-8} - 3.77 \times 10^{-8}$ mol^2/J^2) can not reliably reflect the equilibrium state of the system due to the lower values of the determination coefficients and the much larger values of SSE and χ^2 compared to the Freundlich model.

3.2.2. Kinetic parameters

Kinetic experiments allow the determination of the kinetic parameters that are required to design a sorption process. They are typically carried out to fit the most appropriate sorption reaction rate model. This has been done using three of the most popular kinetic models, such as pseudo-first order (PFO, Equation 9), pseudo-second order (PSO, Equation 10), and intraparticle diffusion (IPD, Equation 11) derived from the Lagergren, Ho and McKay and Weber and Morris assumptions. The linear forms of the above equations are as follows [61,62]:

$$log(q_e - q_t) = log(q_t) - \frac{k_1}{2.303}t \quad (9)$$

Table 5
Isotherm parameters regarding BY2 sorption on EGDMA+VA, EGDMA+VA+20 % St, EGDMA+VA+20 % St/T and EGDMA+VA+20 %St/P.

Isotherm	Parameters	EGDMA+VA	EGDMA+VA +20% St	EGDMA+VA +20% St/T	EGDMA+VA +20% St/P
Freundlich	k_F ($mg^{1-1/n}L^{1/n}/g$)	6.16	6.39	6.56	5.52
	1/n	0.694	0.626	0.731	0.505
	R^2	0.978	0.986	0.997	0.974
	SSE	1.22	0.51	0.48	0.74
	χ^2	0.29	0.22	0.09	0.29
Langmuir	k_L (L/mg)	0.930	1.031	0.62	1.99
	Q_0 (mg/g)	13.91	14.22	18.87	9.75
	R^2	0.924	0.871	0.846	0.910
	SSE	2.10	3.91	2.40	6.73
	χ^2	0.49	0.86	0.46	1.90
Temkin	b_T (J/mol g/mg)	1173	1288	1054	1730
	A (L/mg)	22.79	35.02	20.77	68.92
	R^2	0.887	0.806	0.807	0.871
	SSE	11.20	22.45	0.48	10.50
	χ^2	6.10	18.58	0.09	4.36
Dubinin-Radushkevich	q_m (mg/g)	6.75	5.91	6.44	6.03
	$k_{DR} \times 10^{-8}$ (mol^2/J^2)	3.77	2.37	3.36	2.10
	E (kJ/mol)	3.6	4.59	3.86	4.89
	R^2	0.927	0.807	0.844	0.922
	SSE	23.76	49.81	54.38	21.96
	χ^2	3.44	7.30	6.92	3.54

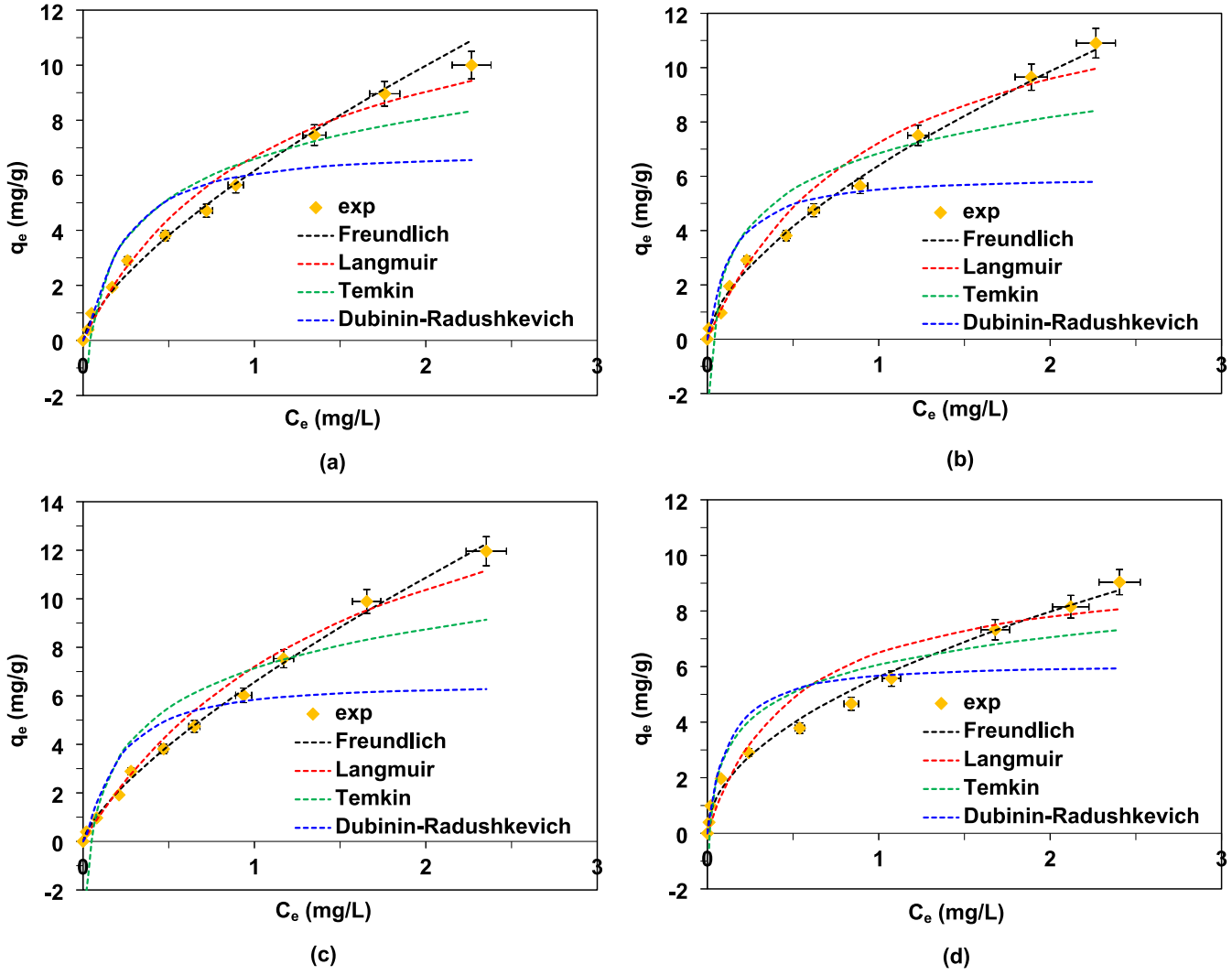

Fig. 10. Fitting of isotherm models to experimental equilibrium data of sorption using (a) EGDMA+VA, (b) EGDMA+VA+20 % St, (c) EGDMA+VA+20 % St/T and (d) EGDMA+VA+20 % St/P.

Table 6
Comparison of isotherm models and calculated parameters applied for BY2 adsorption on different adsorbents based on literature review.

Adsorbent	Conditions	Equilibrium data	Ref.
Natural untreated clay (from Pasinler, Turkey)	a.d. = 0.1 g/L, T=25–45 °C,	Langmuir model: q_e = 833.3–714.28 mg/g	[54]
Bagasse fly ash	a.d. = 1 g/L, T=30 °C, pH=7	Langmuir model: q_e = 31.2 mg/g	[53]
Activated carbon-commercial grade	a.d. = 20 g/L, T=30 °C, pH=7	Langmuir model: q_e = 1.5 mg/g	
Activated carbon-laboratory grade	a.d. = 2 g/L, T=30 °C, pH=7	Langmuir model: q_e = 12.6 mg/g	
Carbon/silica composite	a.d. = 1 g/L, T=20–60°C, pH=7	Freundlich model: k_F=27.37–55.41 $mg^{1-1/n}L^{1/n}/g$	[55]
Hybrid microspheres with co-participated lignin	a.d. = 1 g/L, T=20–60°C	Freundlich model: k_F=11.1–45.7 $mg^{1-1/n}L^{1/n}/g$	[56]
Polystyrene based resins with chloride groups	a.d. = 1 g/L, T=25°C	Freundlich model: k_F=4.56–7.85 $mg^{1-1/n}L^{1/n}/g$	[57]
Diphenylvinylphoshine oxide based resins	a.d. = 1 g/L, T=25°C, pH=8.2	Freundlich model: k_F=13.8 $mg^{1-1/n}L^{1/n}/g$	[58]
Hardened Portland cement paste	a.d. = 0.1 g/L, T=25°C, pH=7	Freundlich model: k_F=81.56 $mg^{1-1/n}L^{1/n}/g$	[59]
Amazon raw clay	a.d. = 1 g/L, T=28°C, pH=5.6	Sips model: q_e = 18.04 mg/g	[60]
EGDMA+VA polymeric adsorbents with modified starch	a.d. = 2.5 g/L, T=25°C, pH=8.3	Freundlich model: k_F=5.62–6.56 $mg^{1-1/n}L^{1/n}/g$	This study

where: a.d. – adsorbent dose, T – temperature.

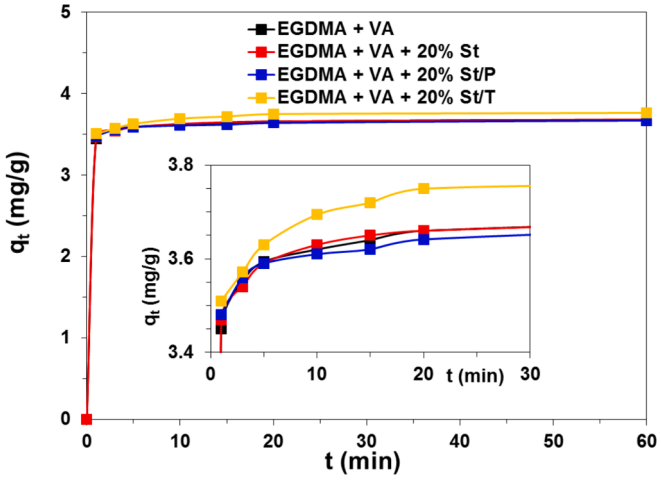

Fig. 11. BY2 adsorption from the solution of the initial concentration of 10 mg/L as a function of time.

$$\frac{t}{q_t} = \frac{1}{k_2 q_e^2} + \frac{1}{q_e} t \tag{10}$$

$$q_t = k_i t^{0.5} \tag{11}$$

where: q_e – the adsorption capacity (mg/g), q_t (mg/g) – the amount of dye adsorbed at time t (min) per unit mass of polymeric microspheres, k_1 (1/min) – the PFO rate constant, k_2 (g/mg min) – the PSO rate constant, k_i (mg/g $min^{0.5}$) – the IPD rate constant.

Fig. 11 presents the uptake of BY2 dye (C_0 = 10 mg/L) by four synthesized adsorbents. BY2 retention by pristine material and starch-modified adsorbents is very rapid. The amount of BY2 sorbed by the obtained materials increased with time and after 25 min the dynamic equilibrium can be observed. The experimental adsorption capacities were found to be in the range of 3.70 to 3.82 mg/g.

The kinetic parameters were calculated using the linear regression method from the slopes and intercepts of the graphs log(q_e-q_t) vs t for the PFO model, t/q_t vs t for the PSO model, and q_t vs $t^{0.5}$ for the IPD model [51,63,64] (**Supplementary materials**, **Fig. S4**), and are listed in Table 7. Based on the values of determination coefficients (R^2 = 0.999) the best fit to the experimental data was found for the PSO model. The pseudo-second order kinetics is applicable in investigated adsorption systems as the plots of t/q_t vs t are a linear relationship (**Supplementary materials**, **Fig. S4 (b)**). The PSO rate constants k_2 were in the range of 1.50 – 2.00 g/mg min. Moreover, not only for pristine material but also for starch-modified adsorbents, no significant differences were found between the calculated (q_e) and experimental ($q_{e,exp}$) amounts of BY2 adsorbed at equilibrium. The model predicts that chemisorption plays a key role in the adsorption process.

According to the PFO model, the rate of change of dye uptake with time is directly proportional to the difference in saturation concentration and the amount of dye sorbed with time, which is usually applicable over the initial stage of adsorption [63,64]. Figure S4 (a) (**Supplementary materials**) shows the PFO dependence as log(q_e–q_t) vs t for BY2 adsorption on the polymeric microspheres containing modified starch. Analyzing the graph, one can see the lack of linearity which causes the experimental $q_{e,exp}$ values not to agree with the calculated q_e data.

The Weber-Morris graph of q_t vs $t^{0.5}$ does not result in straight lines passing through the origin, and the rate of the sorption process can not be considered as being limited by the intraparticle diffusion process [51,63,64] as illustrated in Fig. S4 (c) (**Supplementary materials**). At the same time, the PFO and IPD equations cannot be used to calculate sorption kinetic parameters in the investigated experimental systems as presented in Table 7. The values of the determination coefficients were much smaller than for the PSO model and were in the ranges of 0.719 – 0.782 for the PFO model and 0.777 – 0.895 for the IPD model.

3.2.3. *Auxiliaries impact on BY2 sorption*

Electrolytes and surfactants (also known as auxiliaries in the chemical treatment of textiles) are essential components of dye baths in the textile industry. The type of these substances in the dyeing process depends on the composition of the material to be dyed. They provide suitable conditions for the dye to bond effectively with the fibre. They are consumed only slightly from the dye bath and are discharged into the wastewater practically in the quantities in which they were added to the dye bath. It is therefore important to evaluate their presence on the adsorption yield. They may change the affinity of the adsorbent towards the dye due to different interactions in the aqueous solution. These interactions are influenced by many factors, among which the structures of dye and surfactant are of great importance. C.I. Basic Yellow 2 uptake from the solutions of initial dye concentration 10 mg/L and in the presence of Na_2SO_4 and cationic surfactant CTAB by the polymeric adsorbents with modified starch is presented in Fig. 12. Retention of BY2 was reduced in presence of the CTAB compared with the systems without auxiliaries while Na_2SO_4 does not influence the removal of the dye. Drop of the adsorption capacities of the starch-modified adsorbents from 3.60 to 0.9 mg/g for EGDMA+VA, from 3.62 to 0.6 mg/g for EGDMA+VA+20 % St, from 3.56 to 1.3 mg/g for EGDMA+VA+20 % St/P and from 3.82 to 1.1 mg/g for EGDMA+VA+20 % St/T is caused by competitive adsorption of CTAB compared with BY2 cations.

3.2.4. *Effect of temperature on BY2 sorption*

The effect of temperature on BY2 adsorption on synthesized adsorbents was studied at four various temperatures 298, 308, 318, and 328 K. The dependence of the equilibrium constants (K_C) changing with temperature change was calculated from Eq. (11):

Table 7
Kinetic parameter for BY2 (C_0 = 10 mg/L) sorption by the the EGDMA+VA, EGDMA+VA+20 % St, EGDMA+VA+20 % St/P and EGDMA+VA+20 % St/T microspheres.

Model	Parameter	Adsorbent			
		EGDMA+VA	EGDMA+VA +20 % St	EGDMA+VA +20 % St/T	EGDMA+VA +20 % St/P
PFO	q_e (mg/g)	0.16	0.17	0.27	0.23
	k_1 (1/min)	0.027	0.024	0.010	0.024
	R^2	0.783	0.750	0.719	0.754
PSO	q_e (mg/g)	3.69	3.69	3.68	3.76
	k_2 (g/mg min)	1.94	2.00	1.92	1.50
	R^2	0.999	0.999	0.999	0.999
IPD	k_i (mg/g $min^{0.5}$)	0.042	0.041	0.032	0.054
	R^2	0.780	0.813	0.777	0.895
$q_{e,exp}$ (mg/g)		3.72	3.73	3.70	3.82

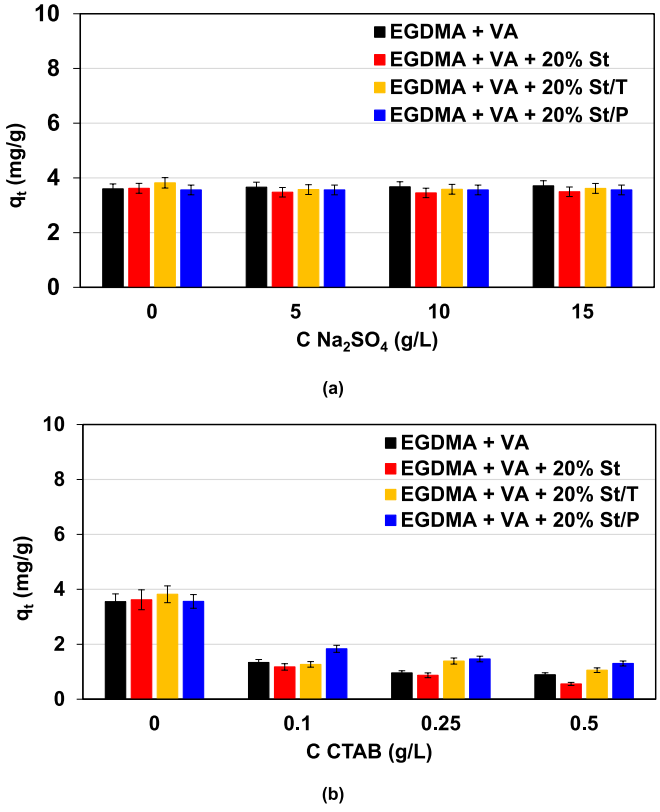

Fig. 12. BY2 adsorption efficiency by on the EGDMA+VA, EGDMA+VA+20 % St, EGDMA+VA+20 % St/P and EGDMA+VA+20 % St/T in the presence of (a) Na_2SO_4 and (b) cationic surfactant CTAB.

$$K_C = \frac{q_e}{C_e} \tag{12}$$

and is presented as $\ln K_C$ versus 1/T (Fig. 13).

The thermodynamic parameters regarding BY2 sorption on starch-modified adsorbents were calculated at four different temperatures using Equations (12–13):

$$\Delta G^o = -RT\ln K_C \tag{12}$$

$$\Delta G^o = \Delta H^o - T\Delta S^o \tag{13}$$

where: ΔG^o – free energy changes (kJ/mol), ΔH^o – free enthalpy changes (kJ/mol), ΔS^o – free entropy changes (kJ/mol K), R – universal gaseous constant (8.314 J/mol K), T – temperature (K).

The negative values of ΔH^o (ranging from 5.02 to 9.61 kJ/mol) reveal that BY2 adsorption on starch-modified polymers is exothermic

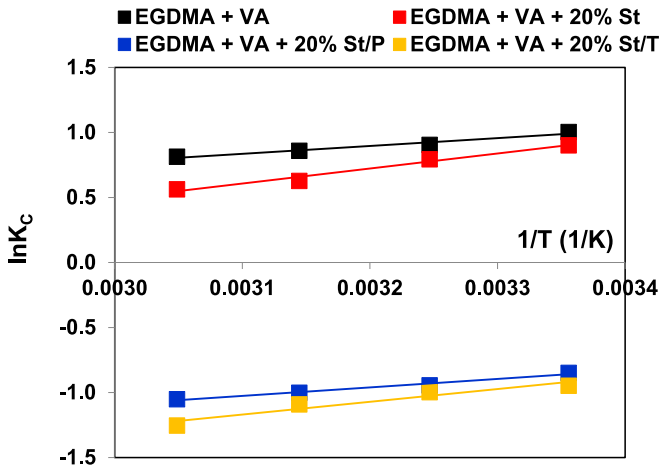

Fig. 13. The thermodynamic equilibrium constant (ln K_C) versus temperature (1/T) for the inesigated system.

process, with negative values of ΔG^o at 298 K, 308 K, 318 K and 328 K indicating spontaneous adsorption of BY2 dye on the EGDMA+VA, EGDMA+VA+20 % St, EGDMA+VA+20 % St/P and EGDMA+VA+20 % St/T. In addition, a less negative value of ΔG^o with a temperature rising from 298 to 328 K demonstrates that a decrease in temperature favors the BY2 uptake. Furthermore, the change in the enthalpy of adsorption for physical nature ranges from −20 to 40 kJ/mol, while chemisorption ranges from −80 to −400 kJ/mol [54]. ΔH^o were calculated to be in the range of −5.02 ÷ −9.61 kJ/mol. The negative values of ΔS^o presented in Table 8 show the decrease in disorderness on BY2 adsorption. Öztürk and Malkoc [54] described retention of BY2 on the untreated clay as exothermic (ΔH^o = 15.91 kJ/mol) and spontaneous (−2.05, −1.44 and −1.17 kJ/mol at 298, 308 and 318 K, respectively) adsorption process of physical nature (5.24 kJ/mol). According to Duarte et al. [60] BY2 adsorption on Amazon raw clay is also spontaneous and exothermic as the negative values of ΔG° (−25.12 to −25.53 kJ/mol) and ΔH° (−18.40 kJ/mol) were calculated. In addition, the values of isosteric heat (ΔH_{st} = −16 ÷ −20 kJ/mol) reveal a predominance of physical interactions [59].

3.2.5. Desorption studies

Regeneration of adsorbents can reduce the risk of environmental contamination with spent adsorbents. Therefore, they are subjected to regeneration by solvent washing, photochemical, or thermal processes, with varying efficiencies [63]. The ability to regenerate the adsorbent is an important aspect of adsorption research and also brings information about the feasibility of using the adsorbent on a technological scale. Both aqueous solutions of hydrochloric acid, sodium chloride, and hydroxide as well as solutions in 50 % v/v methanol were used as eluents to

Table 8
The thermodynamic parameters for BY2 sorption on the EGDMA+VA, EGDMA+VA+20 % St, EGDMA+VA+20 % St/P and EGDMA+VA+20 % St/T.

Adsorbent	ΔH^o (kJ/mol)	ΔS^o (kJ/mol K)	R^2	ΔG^o (kJ/mol)			
				298 K	308 K	318 K	328 K
EGDMA+VA	−5.02	−10.88	0.966	−19.60	−20.01	−20.54	−21.06
EGDMA+VA+20 % St	−9.61	−24.73	0.979	−19.35	−19.72	−19.92	−20.37
EGDMA+VA+20 % St/P	−5.43	−25.35	0.982	−15.01	−15.27	−15.62	−15.97
EGDMA+VA+20 % St/T	−8.15	−35.00	0.926	−14.77	−15.14	−15.38	−15.42

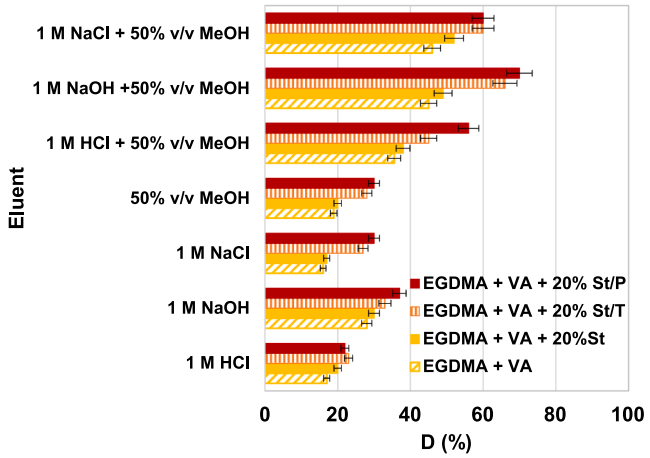

Fig. 14. BY2 desorption from the plymeric adsorbents modified with starch.

overcome interactions of different strengths and nature. As presented in Fig. 14 a significant increase in desorption efficiency was observed when 1 M HCl, 1 M NaCl, and 1 M NaOH solutions were used in 50 % v/v menthol. This is particularly noticeable with the application of the 1 M NaOH+50 % v/v MeOH solutions, desorption yield of BY 2 from the EGDMA+VA, EGDMA+VA+20 % St, EGDMA+VA+20 % St/P and EGDMA+VA+20 % St/T was found to be 45 %, 49 %, 70 % and 66 %, respectively. The addition of methanol enhanced the desorption yield of BY2 and C.I. Basic Blue 3 dyes from functionalized microspheres with co-participate lignin hybrids as described in our previous studies [56]. Xing et al. [65] observed that dye elution such as C.I. Acid Red 18 and C. I. Acid Red 88 from commercial anion exchange membrane was enhanced using ethanol (60 % v/v) addition to 1 M NaCl. Disposal of methanol from eluents can be achieved with a biocenose containing methylotrophic bacteria, which use it as a food source and break it down to carbon dioxide and water [66,67].

4. Conclusions

In the study, the new bioadsorbents based on poly(ethylene glycol-*co*-vinyl acetate dimethacrylate) (EGDMA+VA) and un/modified starch were successfully fabricated as a spherical bead shape (beads diameter: 50–200 μm, surface areas: 176–235 m^2/g, total pores volume: 0.224–0.309 cm^3/g) by suspension polymerization method and applied for BY2 toxic dye removal. The results of ATR/FT-IR, SEM-EDX, and XPS analysis showed that unmodified starch and modified by thiourea or potassium dihydrogen phosphate(V) were successfully incorporated into the EGDMA+VA matrix. The microspheres were thermally resistant, their decomposition took place in two stages and falls within the range of 349–356 and 432–436 °C. Microspheres with starch can be operated up to a temperature of approx. 300 °C. The pH_{pzc} of the starch-modified polymers was found to be in the range of 6.3–7.05. The equilibrium studies revealed that the Freundlich model (k_F=5.62–6.56 $mg^{1-1/n}\ L^{1/n}$, R^2 = 0.974–0.997, SSE=0.48–1.22, χ^2 = 0.09–0.29) can be applied for description of investigated BY2-adsorbents systems rather than Langmuir (R^2 = 0.846–0.924, SSE=2.10–6.73, χ^2 = 0.46–1.9), Temkin (R^2 = 0.806–0.887, SSE=20.48–622.45, χ^2 = 0.09–18.58) or Dubinin-Radushkevich (R^2 = 0.807–0.927, SSE=21.96–54.38, χ^2 = 3.44–7.30). Based on the k_F values the applicability series of starch-modified polymeric adsorbents for BY2 removal can be presented as follows: EGDMA+VA+20 % St/T > EGDMA+VA+20 % St > EGDMA+VA > EGDMA+VA+20 % St/P. The PSO (R^2 = 0.999) model fits kinetic data rather than PFO (R^2 = 0.719–0.783) or IPD (R^2 = 0.777–0.896). Therefore, the mechanism of BY2 uptake by adsorbents can be described as physicochemical with predominant electrostatic interaction between dye cations and dissociated hydroxyl groups of starch-modified polymers. The calculated thermodynamic parameters for BY2 sorption on all fabricated adsorbents revealed the exothermic nature of adsorption and its spontaneousness. Desorption of BY2 from EGDMA+VA+20 % St/T microspheres occurs with an efficiency of 70 % using 1 M NaOH+50 % v/v MeOH. Due to the simplicity of synthesis, satisfactory sorption capacity, and reusability, the newly synthesized polymers containing biodegradable modified starch can be used as potential and sustainable biosorbents for the removal of toxic dyes, especially basic type from dyeing baths and industrial wastewaters with high electrolyte or surfactant content. This manuscript may contribute to further environmental and social implications of sustainable development and preparation of biodegradable adsorbents for treatment of wastewater from other emerging pollutants.

CRediT authorship contribution statement

Monika Wawrzkiewicz: Writing – review & editing, Writing – original draft, Visualization, Validation, Supervision, Software, Methodology, Investigation, Formal analysis, Data curation, Conceptualization. **Beata Podkościelna:** Writing – review & editing, Writing – original draft, Visualization, Validation, Supervision, Methodology, Investigation, Formal analysis, Data curation, Conceptualization. **Bogdan Tarasiuk:** Writing – original draft, Validation, Methodology, Investigation, Data curation, Conceptualization.

Declaration of competing interest

The authors declare that they have no known competing financial interests or personal relationships that could have appeared to influence the work reported in this paper.

Data availability

Data will be made available on request.

Acknowledgements

The authors would like to thank dr Agnieszka Lipke, from the Institute of Chemical Sciences at Maria Curie-Sklodowska University in Lublin for her help in carrying out laboratory work.

Appendix A. Supplementary data

Supplementary data to this article can be found online at https://doi.org/10.1016/j.measurement.2024.115556.

References:

[1] L. Yang, Y. Sun, R. Yu, P. Huang, Q. Zhou, H. Yang, S. Lin, H. Zeng, J. Hazard. Mater. 469 (2024) e134101.
[2] Y. Wei, A. Ding, Y. Chen, A novel titanium sulfate modified poly-magnesium-silicate coagulant with improved pH range for dye removal, J. Environ. Manage. 343 (2023) e118168.
[3] C. Hessel, C. Allegre, M. Maisseu, F. Charbit, P. Moulin, Guidelines and legislation for dye house effluents, J. Environ. Manage. 83 (2007) 171–180.
[4] K. Turhan, Z. Turgut, Decolorization of direct dye in textile wastewater by ozonization in a semi-batch bubble column reactor, Desalination 242 (2009) 256–263.
[5] R. Al-Tohamy, S.S. Ali, F. Li, K.M. Okasha, Y.-A.-G. Mahmoud, T. Elsamahy, H. Jiao, Y. Fu, J. Sun, A critical review on the treatment of dye-containing wastewater: ecotoxicological and health concerns of textile dyes and possible remediation approaches for environmental safety, Ecotoxicol. Environ. Saf. 231 (2022) e113160.
[6] C.C.J. Azevedo, R. de Oliveira, P. Suares-Rocha, D. Sousa-Moura, A. Tianwen Li, C. K. Grisolia, G. de Aragão Umbuzeiro, C.C. Montagner, Auramine dyes induce toxic effects to aquatic organisms from different trophic levels: an application of predicted non-effect concentration (PNEC), Environ. Sci. Pollut. Res. 28 (2021) 1866–1877.
[7] M. Bahrami, M.J. Amiri, F. Bagheri, Optimization of crystal violet adsorption by chemically modified potato starch using response surface methodology, Pollution 6 (2020) 159–170.
[8] M. Bahrami, M. Javad Amiri, F. Bagheri, Optimization of the lead removal from aqueous solution using two starch based adsorbents: design of experiments using response surface methodology (RSM), J. Environ. Chem. Eng. 7 (2019) e102793.
[9] V. Katheresan, J. Kansedo, S.Y. Lau, Efficiency of various recent wastewater dye removal methods: a review, J. Environ. Chem. Eng. 6 (2018) 4676–4697.
[10] G.L. Dotto, J.M.N. Santos, I.L. Rodrigues, R. Rosa, F.A. Pavan, E.C. Lima, Adsorption of Methylene Blue by ultrasonic surface modified chitin, J. Colloid Interface Sci. 446 (2015) 133–140.
[11] T. Aziz, F. Haq, A. Farid, M. Kiran, S. Faisal, A. Ullah, N. Ullah, A. Bokhari, M. Mubashir, L. Fatt Chuah, P. Loke Show, Challenges associated with cellulose composite material: facet engineering and prospective, Environ. Res. 223 (2023) e115429.
[12] T. Aziz, A. Farid, F. Haq, M. Kiran, A. Ullah, K. Zhang, C. Li, S. Ghazanfa, H. Sun, R. Ullah, A. Ali, M. Muzammal, M. Shah, N. Akhtar, S. Selim, N. Hagagy, M. Samy, K.S. Al Jaouni, A review on the modification of cellulose and its applications, Polymers 14 (2022) e3206.
[13] M. Jiang, Y. Ma, T. Wang, N. Niu, L. Chen, Hybrid lignin particles via ion-crosslinked for selective removal of anionic dyes from water, Int. J. Biol. Macromol. 238 (2023) e124080.
[14] A. Ali Aslam, S. Ul Hassan, M. Haris Saeed, O. Kokab, Z. Ali, M. Shahid Nazir, W. Siddiqi, A. Ali Aslam, Cellulose-based adsorbent materials for water remediation: harnessing their potential in heavy metals and dyes removal, J. Clean. Prod. 421 (2023) e138555.
[15] J. Zheng, T. Aziz, H. Fan, F. Haq, U.K. Fazal, U. Farman, U. Roh, S.K. Bakhtar, J. Noor Wei, Synergistic impact of cellulose nanocrystals with multiple resins on thermal and mechanical behavior, Z. Phys. Chem. 235 (2021) 1247–1262.
[16] Ch. Li, H. Fan, T. Aziz, C. Bittencourt, L. Wu, D.-Y. Wang, P. Dubois, Biobased epoxy resin with low electrical permissivity and flame retardancy: from environmental friendly high-throughput synthesis to properties, ACS Sustain. Chem. Eng. 6 (2018) 8856–8867.
[17] X. Zhang, Y. Cai, X. Zhang, T. Aziz, H. Fan, C. Bittencourt, Synthesis and characterization of eugenol-based silicone modified waterborne polyurethane with excellent properties, J. Appl. Polym. Sci. 138 (2021) e50515.
[18] K. Fang, L. Deng, J. Yin, T. Yang, J. Li, W. He, Recent advances in starch-based magnetic adsorbents for the removal of contaminants from wastewater: a review, Int. J. Biol. Macromol. 218 (2022) 909–929.
[19] J.I. Enrione, S.E. Hill, J.R. Mitchell, Sorption behaviour of mixtures of glycerol and starch, J. Agric. Food Chem. 55 (2007) 2956–2963.
[20] T. Oniszczuk, S. Muszyński, A. Kwaśniewska, The evaluation of sorption properties of thermoplastic starch pellets, Przemysł Chemiczny 94 (2015) 1752–1756, in Polish.
[21] T. Jiang, Q. Duan, J. Zhu, H. Liu, L. Yu, Starch-based biodegradable materials: challenges and opportunities, Advanced Industrial and Engineering Polymer Research 3 (2020) 8–18.
[22] A. Das, N. Sit, Modification of taro starch and starch nanoparticles by various physical methods and their characterization, Starch-Stärke 73 (2021) e2000227.
[23] N. Wang, C. Li, D. Miao, H. Hou, Y. Dai, Y. Zhang, W. Wang, The effect of non-thermal physical modification on the structure, properties and chemical activity of starch: a review, Int. J. Biol. Macromol. 251 (2023) e126200.
[24] F. Haq, H. Yu, L. Wang, L. Teng, M. Haroon, R.U. Khan, S. Mehmood, R.S. Ullah, A. Kan, A. Nazir, Advances in chemical modifications of starch and their applications, Carbohydr. Res. 476 (2019) 12–35.
[25] A.M. Farag, H.H. Sokker, E.M. Zayed, F.A. Nour Eldien, N.M. Abd Alrahman, Removal of hazardous pollutants using bifunctional hydrogel obtained from modified starch by grafting copolymerization, Int. J. Biol. Macromol. 120 (2018) 2188–2199.
[26] B. Zhang, D. Cui, M. Liu, H. Gong, Y. Huang, F. Han, Corn porous starch: preparation, characterization and adsorption property, Int. J. Biol. Macromol. 50 (2012) 250–256.
[27] Y. Zhong, J. Xu, X. Liu, L. Ding, B. Svensson, K. Herburger, K. Guo, C. Pang, A. Blennow, Recent advances in enzyme biotechnology on modifying gelatinized and granular starch, Trends Food Sci. Technol. 123 (2022) 343–354.
[28] T. Aziz, H. Fan, F. Haq, F.U. Khan, A. Numan, A. Ullah, N. Wazir, Facile modification and application of cellulose nanocrystals, Iran. Polym. J. 28 (2019) 707–724.
[29] Q. Tan, X. Jia, R. Dai, H. Chang, M. Wai Woo, H. Chen, Synthesis of a novel magnetically recyclable starch-based adsorbent for efficient adsorption of crystal violet dye, Sep. Purif. Technol. 320 (2023) e124157.
[30] X. Dang, Z. Yu, M. Yang, M. Wai Woo, Y. Song, X. Wang, H. Zhang, Sustainable electrochemical synthesis of natural starch-based biomass adsorbent with ultrahigh adsorption capacity for Cr(VI) and dyes removal, Sep. Purif. Technol. 288 (2022) e120668.
[31] T. Aziz, A. Ullah, H. Fan, R. Ullah, F. Haq, F.U. Khan, M. Iqbal, J. Wei, Cellulose nanocrystals applications in health, medicine and catalysis, J. Polym. Environ. 29 (2021) 2062–2071.
[32] S. Mehmood, F. Haq, M. Kiran, Cyclo-matrix poly(cyclotriphosphazene-co-kaempferol) microspheres: synthesis, characterization, EPR study and their controlled drug release application, J. Polym. Environ. 31 (2023) 4817–4828.
[33] S. Lawchoochaisakul, P. Monvisade, P. Siriphannon, Cationic starch intercalated montmorillonite nanocomposites as natural based adsorbent for dye removal, Carbohydr. Polym. 253 (2021) e117230.
[34] D. Sarmah, N. Karak, Double network hydrophobic starch based amphoteric hydrogel as an effective adsorbent for both cationic and anionic dyes, Carbohydr. Polym. 242 (2020) e116320.
[35] X. Wang, A. Zhang, M. Chen, M.K. Seliem, M. Mobarak, Z. Diao, Z. Li, Adsorption of azo dyes and Naproxen by few-layer MXene immobilized with dialdehyde starch nanoparticles: adsorption properties and statistical physics modeling, Chem. Eng. J. 473 (2023) e145385.
[36] H. Hosseinzadeh, S. Ramin, Fabrication of starch-graft-poly(acrylamide)/graphene oxide/hydroxyapatite nanocomposite hydrogel adsorbent for removal of malachite green dye from aqueous solution, Int. J. Biol. Macromol. 106 (2018) 101–115.
[37] S. Noreen, H.N. Bhatti, M. Iqbal, F. Hussain, F. Malik Sarim, Chitosan, starch, polyaniline and polypyrrole biocomposite with sugarcane bagasse for the efficient removal of Acid Black dye, Int. J. Biol. Macromol. 147 (2020) 439–452.
[38] I. Ihsanullah, M. Bilal, A. Jamal, Recent developments in the removal of dyes from water by starch-based adsorbents, Chem. Rec. 22 (2022) e 202100312.
[39] N.M. Mahmoodi, M.S.M.A. Roudaki, K. Didehban, M.R. Saeb, Ethylenediamine/glutaraldehyde-modified starch: a bioplatform for removal of anionic dyes from wastewater, Korean J. Chem. Eng. 36 (2019) 1421–1431.
[40] A. Grover, I. Mohiuddin, A.K. Malik, J.S. Aulakh, K. Vikrant, K.-H. Kim, R.J. C. Brown, Magnesium/aluminum layered double hydroxides intercalated with starch for effective adsorptive removal of anionic dyes, J. Hazard. Mater. 424 (2022) e127454.
[41] A. Rangelov, S. Stoyanov, L. Arnaudov, T. Spassov, Novel mechanochemical approach for wheat starch-LPC complex formation, J. Cereal Sci. 76 (2017) 72–75.
[42] Y.J. Zhang, L.L. Chen, K.X. Yu, Y.Y. Dai, L. Wang, X.Z. Ding, H.X. Hou, W.T. Wang, H. Zhang, X.Y. Li, H.Z. Dong, Mechanochemical effect of ultrasound on sweet potato starch and its influence mechanism on the quality of octenyl succinic anhydride modified starch, Food Sci. Technol. Int. 26 (3) (2020) 254–264.
[43] V. Burmistrov, I. Lipatova, I. Trifonova, N. Losev, Y. Rodicheva, O. Koifman, Polyurethane and styrene-acrylic copolymer as modifiers for starch composites preparation under the mechanochemical activation: a multifactorial approach, Mater. Lett. 322 (2022) e132502.
[44] B. Podkościelna, B. Gawdzik, A. Bartnicki, Use of a new methacrylic monomer, 4,4'-di(2-hydroxy-3-methacryloyloxypropoxy)benzophenone, in the synthesis of porous microspheres, J. Polym. Sci., Part A: Polym. Chem. 44 (2006) 7014–7026.
[45] B. Podkościelna, B. Gawdzik, Influence of diluent compositions on the porous structure of methacrylate derivatives of aromatic diols and divinylbenzene, Appl. Surf. Sci. 256 (2010) 2462–2467.
[46] B. Gawdzik, B. Podkościelna, A. Bartnicki, Synthesis, structure and properties of new methacrylic derivatives of naphthalene-2,3-diol, J. Appl. Polym. Sci. 102 (2006) 1886–1895.
[47] M. Wawrzkiewicz, B. Podkościelna, P. Podkościelny, Application of functionalized DVB-co-GMA polymeric microspheres in the enhanced sorption process of hazardous dyes from dyeing baths, Molecules 25 (2020) e5247.
[48] P. Kongseng, P. Amornpitoksuk, S. Chantarak, ZnO/Cassava starch-based hydrogel composite for effective treatment of dye-contaminated wastewater, Macromol. Mater. Eng. 308 (2023) e2200481.
[49] C. Cagnin, B.M. Simões, F. Yamashita, G.M. de Carvalho, M.V. Eiras Grossmann, pH sensitive phosphate crosslinked films of starch-carboxymethyl cellulose, Polym. Eng. Sci. 61 (2021) 388–396.
[50] M. Mozaffari Majd, V. Kordzadeh-Kermani, V. Ghalandari, A. Askari, M. Sillanpää, Adsorption isotherm models: a comprehensive and systematic review (2010–2020), Sci. Total Environ. 812 (2022) e151334.
[51] S.Z. Mohammadi, N. Mofidinasab, M.A. Karimi, A. Beheshti, Removal of methylene blue and Cd(II) by magnetic activated carbon–cobalt nanoparticles and its application to wastewater purification, Int. J. Environ. Sci. Technol. 17 (2020) 4815–4828.
[52] O.P. Murphy, M. Vashishtha, P. Palanisamy Vasanth, K. Kumar, A review on the adsorption isotherms and design calculations for the optimization of adsorbent mass and contact time, ACS Omega 8 (2023) 17407–17430.
[53] I.D. Mall, V.C. Srivastava, N.K. Agarwal, Adsorptive removal of auramine-O: kinetic and equilibrium study, J. Hazard. Mater. 143 (2007) 386–395.

[54] A. Öztürk, E. Malkoc, Adsorptive potential of cationic Basic Yellow 2 (BY2) dye onto natural untreated clay (NUC) from aqueous phase: mass transfer analysis, kinetic and equilibrium profile, Appl. Surf. Sci. 299 (2014) 105–115.
[55] M. Wiśniewska, M. Wawrzkiewicz, M. Onyszko, M. Medykowska, A. Nosal-Wiercińska, V. Bogatyrov, Carbon-silica composite as adsorbent for removal of hazardous C.I. Basic Yellow 2 and C.I. Basic Blue 3 dyes, Materials 14 (2021) e3245.
[56] M. Wawrzkiewicz, B. Podkościelna, T. Jesionowski, Ł. Klapiszewski, Functionalized microspheres with co-participated lignin hybrids as a novel sorbents for toxic C.I. Basic Yellow 2 and C.I. Basic Blue 3 dyes removal from textile sewage, Ind. Crop. Prod. 180 (2022) e114785.
[57] M. Wawrzkiewicz, B. Podkościelna, Innovative polymer microspheres with chloride groups synthesis, characterization and application for dye removal, Processes 10 (2022) e1568.
[58] M. Wawrzkiewicz, S. Frynas, B. Podkościelna, Synthesis and characterization of phosphorus-containing sorbent for basic dye removal, Molecules 28 (2023) e6731.
[59] M.H. Rasoulifard, F. Haddai Esfahlani, H. Mehrizadeh, N. Sehati, Removal of C.I. Basic Yellow 2 from aqueous solution by low-cost adsorbent: hardened paste of Portland cement, Environ. Technol. 31 (2010) 277–284.
[60] E.D.V. Duarte, W.T. Vieira, R.O. Góes, L.E.C. de Azevedo, M.G.A. Vieira, M.G.C. da Silva, S.M.L. de Carvalho, Amazon raw clay as a precursor of a clay-based adsorbent: experimental study and DFT analysis for the adsorption of Basic Yellow 2 dye, Environ. Sci. Pollut. Res. 30 (2023) 62602–62624.
[61] Y.S. Ho, G. McKay, Sorption of dye from aqueous solution by peat, Chem. Eng. J. 70 (1998) 115–124.
[62] J.P. Vareda, On validity, physical meaning, mechanism insights and regression of adsorption kinetic models, J. Mol. Liq. 376 (2023) e121416.
[63] S.Z. Mohammadi, Z. Safari, N. Madady, A novel Co_3O_4@SiO_2 magnetic nanoparticle-nylon 6 for high efficient elimination of Pb(II) ions from wastewater, Appl. Surf. Sci. 514 (2020) e145873.
[64] S.Z. Mohammadi, N. Mofidinasab, M.A. Karimi, F. Mosazadeh, Fast and efficient removal of Pb(II) ion and malachite green dye from wastewater by using magnetic activated carbon–cobalt nanoparticles, Water Sci. Technol. 82 (2020) 829–842.
[65] T. Xing, H. Kai, G. Chen, Study of adsorption and desorption performance of acid dyes on anion exchange membrane, Color. Technol. 128 (2012) 295–299.
[66] P. Kaszycki, K. Czechowska, P. Petryszak, J. Międzobrodzki, B. Pawlik, H. Kołoczek, Methylotrophic extremophilic yeast Trichosporon sp.: a soil-derived isolate with potential applications in environmental biotechnology, Acta Biochim. Pol. 53 (2006) 463–473.
[67] P. Kaszycki, H. Koloczek, Biodegradation of formaldehyde and its derivatives in industrial wastewater with methylotrophic yeast *Hansenula polymorpha* and with the yeast-bioaugmented activated sludge, Biodegradation 13 (2002) 91–99.